PLOS GENETICS

RESEARCH ARTICLE

Quantitative mapping of mRNA 3' ends in *Pseudomonas aeruginosa* reveals a pervasive role for premature 3' end formation in response to azithromycin

Salini Konikkat[1], Michelle R. Scribner[2], Rory Eutsey[1], N. Luisa Hiller[1], Vaughn S. Cooper[2], Joel McManus[1]*

1 Department of Biological Sciences, Carnegie Mellon University, Pittsburgh, Pennsylvania, United States of America, **2** Department of Microbiology and Molecular Genetics, University of Pittsburgh, Pittsburgh, Pennsylvania, United States of America

* mcmanus@andrew.cmu.edu

Abstract

Pseudomonas aeruginosa produces serious chronic infections in hospitalized patients and immunocompromised individuals, including patients with cystic fibrosis. The molecular mechanisms by which *P. aeruginosa* responds to antibiotics and other stresses to promote persistent infections may provide new avenues for therapeutic intervention. Azithromycin (AZM), an antibiotic frequently used in cystic fibrosis treatment, is thought to improve clinical outcomes through a number of mechanisms including impaired biofilm growth and quorum sensing (QS). The mechanisms underlying the transcriptional response to AZM remain unclear. Here, we interrogated the *P. aeruginosa* transcriptional response to AZM using a fast, cost-effective genome-wide approach to quantitate RNA 3' ends (3pMap). We also identified hundreds of *P. aeruginosa* genes with high incidence of premature 3' end formation indicative of riboregulation in their transcript leaders using 3pMap. AZM treatment of planktonic and biofilm cultures alters the expression of hundreds of genes, including those involved in QS, biofilm formation, and virulence. Strikingly, most genes downregulated by AZM in biofilms had increased levels of intragenic 3' ends indicating premature transcription termination, transcriptional pausing, or accumulation of stable intermediates resulting from the action of nucleases. Reciprocally, AZM reduced premature intragenic 3' end termini in many upregulated genes. Most notably, reduced termination accompanied robust induction of *obgE*, a GTPase involved in persister formation in *P. aeruginosa*. Our results support a model in which AZM-induced changes in 3' end formation alter the expression of central regulators which in turn impairs the expression of QS, biofilm formation and stress response genes, while upregulating genes associated with persistence.

Competing interests: The authors have declared that no competing interests exist.

Author summary

Pseudomonas aeruginosa is a common source of hospital-acquired infections and causes prolonged illness in patients with cystic fibrosis. *P. aeruginosa* infections are often treated with the macrolide antibiotic azithromycin, which changes the expression of many genes involved in infection. By examining such expression changes at nucleotide resolution, we found azithromycin treatment alters the locations of mRNA 3' ends suggesting most downregulated genes are subject to premature 3' end formation. We further identified candidate RNA regulatory elements that *P. aeruginosa* may use to control gene expression. Our work provides new insights in *P. aeruginosa* gene regulation and its response to antibiotics.

Introduction

The Gram-negative bacterium *Pseudomonas aeruginosa* (*P. aeruginosa*) is an important opportunistic pathogen in humans. It is a leading cause of hospital-associated pneumonia [1–6]. *P. aeruginosa* infections are associated with increased morbidity and risk of death in patients with pulmonary disorders such as cystic fibrosis (CF), chronic obstructive pulmonary disease (COPD), and diffuse parabronchiolitis (DPB). *P. aeruginosa* readily forms aggregates or biofilms that are thought to exacerbate disease progression, and contribute to antibiotic resistance and the persistent nature of *P. aeruginosa* infections [7–11]. For example, in the lungs of patients with cystic fibrosis, *P. aeruginosa* biofilms cause continual damage to the airways by recurrent infection, inflammation, and airway obstruction [12]. Due to their clinical importance, understanding the regulation of biofilms has become a major focus of *P. aeruginosa* research.

Sub-inhibitory concentrations of the macrolide antibiotic azithromycin (AZM) improves clinical outcomes in patients with cystic fibrosis, diffuse panbronchiolitis (DPB) and chronic obstructive pulmonary disease (COPD) [13–17]. In mouse models of *P. aeruginosa* infection, including a CF model, AZM reduced bacterial load and improved lung pathology [18, 19]. These effects were attributed to the interference with quorum sensing (QS), suppression of virulence factors, and attenuation of host inflammatory responses. Previous studies demonstrated that AZM targets QS by an uncertain mechanism, which in turn is proposed to control biofilm formation and virulence factor production [20–29]. Consistent with these biological effects, AZM treatment changes the transcript levels of genes involved in QS, virulence factor production, and oxidative stress [2, 20–29]. For example, AZM downregulates the expression of components of the *lasI/lasR* and *rhlI/rhlR* QS systems as well as QS-controlled genes coding for virulence factors such as elastase, flagellar motility factors, and rhamnolipid synthesis [2, 20–22, 25, 27–29]. AZM also downregulates QS-regulated oxidative stress response genes including catalase *katA* and superoxide dismutase *sodB* [25, 30]. While these pathways clearly respond to AZM, the underlying mechanisms remain unclear, particularly in biofilms.

AZM binds near the peptidyl transferase center on the large subunit of bacterial ribosomes and disrupts translation elongation by hindering the passage of newly synthesized polypeptides through the polypeptide exit tunnel [31–35]. Translation inhibition is hence thought to account for QS inhibition, which in turn inhibits biofilm formation and virulence gene expression by AZM in *P. aeruginosa*. Because transcription elongation and mRNA translation are spatio-temporally coupled in bacteria [36–39], the translation stalling caused by AZM could directly alter the production of full-length transcripts from QS genes and transcriptional regulators of the stress response. The extent of reduced transcriptional processivity due to AZM

treatment remains an important unresolved question because methods used in previous studies lacked the resolution to differentiate between premature and full-length mRNA transcripts.

RNA 3' end mapping allows genome-wide identification of RNA 3'-OH ends [40] and quantitation of differential gene expression [41, 42]. RNA molecules with free 3'-OH ends include both full length and premature transcripts resulting from intrinsic or factor-dependent transcription termination, transcriptional pauses and stable intermediates produced by ribonucleases [40, 43–45]. Bacteria often employ conditional transcription termination in their transcript leaders to regulate expression in response to drugs, metabolites, and stresses [46–51]. *Cis*-regulatory elements that use premature transcription termination include transcription attenuators and riboswitches, often collectively referred to as riboregulators. Their mechanisms of action involve formation of alternate RNA structures that promote full length transcript synthesis (anti-terminator) or effect premature transcription termination (terminator). The activities of riboregulators are often mediated by interaction of the nascent transcript with small molecules, ribosomes, tRNAs, or regulatory proteins. As such, riboregulators are potential therapeutic targets, and may provide synthetic biology applications [52–55]. Since conditional premature transcription termination regulates biofilm formation, virulence, and expression of antibiotic resistance genes in other bacteria [40, 51, 56, 57], efforts to identify and characterize genes likely to be controlled by riboregulators in *P. aeruginosa* would be beneficial.

In this study, we employed a modification of the genome-wide 3' end mapping approach Term-Seq [40], which we call 3pMap (Fig 1), to characterize the transcriptional landscape of *P. aeruginosa* and the acute effects of clinically relevant sub-inhibitory concentrations of AZM on gene expression. We examined differential gene expression in planktonic and biofilm cultures of *P. aeruginosa* in response to AZM. AZM altered the expression of over two hundred genes in each condition, including key factors involved in QS, biofilm formation, virulence factor production, and stress responses. Notably, most genes downregulated in response to AZM in biofilms showed increased intragenic 3' end formation, indicating a role for the antibiotic in regulating transcription. Furthermore, AZM treatment strongly induced the peristence gene *obgE*, accompanied by a corresponding decrease in premature 3' end formation in its transcript leader. Together, our results provide novel insights into transcriptional regulation in *P. aeruginosa* and support a model in which AZM-induced changes in premature 3' end formation alter the expression of key transcriptional modulators and structural genes involved in QS, virulence, stress response, and persistence.

Methods

Strains and culture conditions

The effects of AZM on both planktonic cells and biofilms of a UCBPP-PA14 strain isolate (genome at NCBI GEO under accession GSE173073) were investigated. Populations from freezer stock were revived by culturing overnight in LB broth at 37°C with shaking at 300 RPM to an optical density (OD_{600}) of 1.0. For planktonic cells, this culture was diluted to OD_{600} 0.1 in 5 mL LB broth and grown to a final OD_{600} of 0.47 (~3 hours shaking at 37°C). A subinhibitory concentration of AZM (0.5 μg/ml final concentration) was added to three cultures (S1 Fig). Three cultures without AZM were used as negative controls. The cultures were incubated for an additional 20 minutes at 37°C. One volume of RNA stabilization solution (5.3M ammonium sulfate, 20 mM EDTA, 25 mM sodium citrate, pH 5.2) was added and the cells were pelleted by centrifugation at 2,500xg for 10 minutes. The supernatants were discarded and the pellets were frozen at -20°C for RNA extraction. For biofilms, a mid-log phase PA14 culture was diluted to an optical density of 0.05 into six-well plates (one plate per
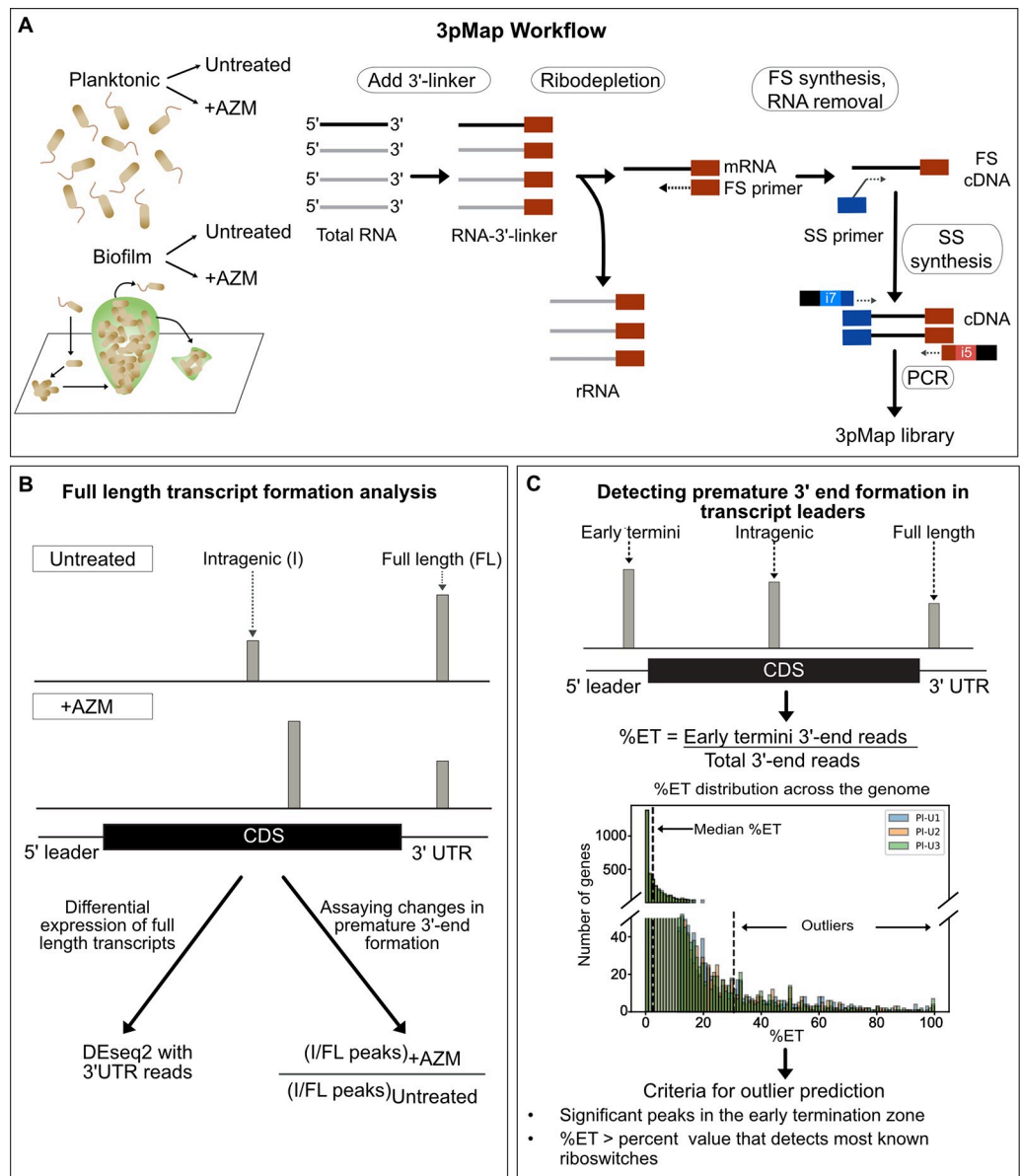
Fig 1. 3pMap workflow and data analysis. (A) 3pMap library synthesis. A 3' adapter is ligated to total RNA, followed by rRNA depletion. The cDNA is generated by reverse transcription with oligos containing sequences complementary to the adapter (first strand, FS) and to random priming sites (second strand, SS). The cDNA libraries are PCR amplified to generate Illumina sequencing libraries. **(B)** Assaying changes in full length transcript synthesis. 3' end reads and peaks were categorized as intragenic (I) and full length (FL) depending on their locations. Differential changes in gene expression were measured using DEseq2 of all 3' end reads (see Methods). Relative changes in premature 3' end formation were measured by comparing the I/FL peaks in AZM-treated vs. untreated samples. **(C)** Predicting RNA regulatory elements in transcript leader neighborhood. 3' end reads are assigned to genes /operons and categorized as early termini (transcript leader + 40 nucleotides) (ET), intragenic (I), and 3'UTR or full length (FL) reads. Genes with significant 3' end peaks in the ET zone and %ET >30 are considered outlier candidates.

https://doi.org/10.1371/journal.pgen.1009634.g001

culture) incubated at 37˚C for 24 hours. The media was removed and replaced with or without AZM (0.5 µg/ml) and incubated at 37˚C for 3 hours. The media was removed and 750 µl RNA stabilization solution was added to each well. The biofilms were scraped from the wells and the cells were pelleted by centrifugation at 2500xg for 10 minutes. The supernatants were discarded and samples were saved at -20˚C until RNA extraction.

RNA extraction and DNase treatment

Total RNA was extracted using the Quick-RNA Fungal/Bacterial Miniprep kit (Zymo Research R2010) according to the manufacturer's instructions. To remove any contaminating genomic DNA, 20–40 μg of total RNA was incubated with 6 units of TURBO-DNase (Thermo Fisher Scientific AM2238), 1X TURBO DNase buffer, and 20 units of SUPERase-In RNase inhibitor in a 1 ml reaction for 1 hour at 37°C. The RNA was re-isolated using acid-phenol, ethanol precipitated, and resuspended in nuclease-free water. The absence of contaminating DNA was confirmed by the absence of a GAPDH PCR product, using genomic DNA as a positive control for the PCR.

High-throughput sequencing library preparation using 3pMAP

3'-linker addition and rRNA depletion

To reduce secondary structure, a 5 μl reaction containing 2 μg of RNA and 375 ng of universal miRNA 3'-cloning linker (New England Biolabs S1315S) was heated at 80°C for 2 minutes and placed on ice. The RNA was ligated to the 3'-linker by incubating the mix overnight at 16°C in a 20 μl reaction containing 12.5% PEG800, 10% DMSO, 1X T4 RNA Ligase buffer, 20 units SUPERase-In RNase inhibitor, and 200 units of T4 RNA Ligase 2, truncated K227Q (New England Biolabs M0351S). The RNA was precipitated with 3 volumes of ethanol, 1/10th volume of 3M sodium acetate (pH 5.2) and 20 μg of glycogen at -80°C for 1 hour. Ribosomal RNA (rRNA) depletion was performed using the Ribo-Zero rRNA removal kit for bacteria (Illumina MRZMB126) as per the manufacturer's instructions, and ethanol precipitated as discussed above.

High-throughput sequencing library synthesis and sequencing

Strand-specific 3pMap libraries were prepared using the QuantSeq Flex Targeted RNA-seq kit (Lexogen SKU:035.24) with the following modifications. Oligonucleotides used for library synthesis are listed below. First strand cDNA synthesis was performed as per the manufacturer's instruction using 5 μl of 2.5 μM custom first strand synthesis primer mix containing partial Illumina Read 1 adapter (below). Following the first strand synthesis, RNA was removed, and the second strand of cDNA was synthesized using SS1X mix and custom second strand synthesis primer with Illumina Read 2 sequence. Half the purified cDNA was used as a template for PCR amplification using barcoded primers provided with the kit. The library concentrations were quantified using a Qubit dsDNA high sensitivity assay (ThermoFisher Scientific Q32854) and sizes were estimated on a Tapestation high sensitivity DNA ScreenTape (Aglient). The libraries were sequenced on an Illumina NextSeq 500 platform in a single-read, 75-nucleotide run as per the manufacturer's instructions.

Oligonucleotides for library preparation

First Strand Synthesis Mix (equimolar mix of three primers used for first strand synthesis):
    3PUTR-FS-N-Read1 5'-CACGACGCTCTTCCGATCTNATTGATGGTGCCTACAG-3'
    3PUTR-FS-NN-Read1 5'-CACGACGCTCTTCCGATCTNNATTGATGGTGCCTACAG-3'
    3PUTR-FS-NNN-Read1 5'-CACGACGCTCTTCCGATCTNNNATTGATGGTGCCTACAG-3'
    Random Second Strand Synthesis (SS) Primer
    RandomSS-Read2 5'-GTTCAGACGTGTGCTCTTCCGATCTNNNNNNNNNNNNN-3'

Data processing

Aligning reads to the genome and identifying significant peaks

Reads were first trimmed to remove adapter sequences. 5' ends were trimmed with a custom Perl script (5p-trimmer.pl), which removed 15–17 nucleotides preceding "CAG", then 3' ends were trimmed using Cutadapt (v. 1.9.1; parameters -a AGATCGGAAGAGC -m 25) and aligned to our UCBPP-PA14 genome sequence (NCBI GEO, see above) using Bowtie2 (v 2.1.0, default parameters) to obtain the genomic coordinates for the 3'-ends of reads [58, 59]. 3pMap is strand specific, such that reads map to the strand from which they were transcribed. We used a custom Perl script, Map3p-seq-peaks.pl, to compare aligned 3' end locations to an expected Poisson distribution of random 3' ends in 50 nucleotide windows. Candidate peaks required a raw p-value $< 5 \times 10^{-5}$, > 5-fold more reads than the average within the window, and a minimum of 5 total reads per peak. Strand specific peak files for each replicate were combined and RNA 3' peaks that are present in at least two of three sample replicates were identified using a combination of bedtools functions [60] (MakeSignificantPeaksFile.sh). These peaks are referred to as significant peaks in further analyses.

Bioinformatic prediction of Rho-independent terminators in *P.* aeruginosa

Rho-independent terminators in the *P. aeruginosa* genome were predicted using ARNold, a web-tool that combines two prediction algorithms Erpin and RNAmotif [61]. Due to limitations on the input file size, *P. aeruginosa* genome was split into two halves. The genomic coordinates for predicted Rho-independent terminators in the second output file were compiled using a Python script and a mergebed bedtools operation was performed in a strand-specific manner to obtain a 6-column file with coordinates for Rho-independent terminators (S1 Table).

Genome-browser images

Integrated Genome Viewer [62] (IGV) images were exported as Scaled Vector Graphics (.svg) images and edited on Adobe Illustrator or Affinity Designer to obtain simplified views. Views for negative strand genes were inverted using mirror display option for the ease of visualization. IGV tracks show the reads present in the same strand as the gene of interest, using autoscale. The genomic coordinates for the IGV snapshots are included in the images. 3' end read counts for samples are indicated above the tracks corresponding to the sample.

Associating 3' end reads with *P. aeruginosa* genes

For analysing the ability of 3pMap to accurately detect RNA 3' ends, 3' end reads within 400 nucleotides of genes were associated with the coordinates in.gff file using the bedtools windowbed function. The 3' end significant peaks were associated with tRNAs and mRNAs if they were (a) intragenic located within the gene boundaries or (b) intergenic–n nucleotides downstream of the annotated 3' end and does not overlap into the next gene on the same strand (n = 400 for mRNAs and n = 100 for tRNAs as the intergenic spaces between these genes and their downstream genes were shorter). For remaining steps in the analysis, genomic coordinates of *P.aeruginosa* transcript leaders (5'-UTRs) and transcriptional unit boundaries were obtained using LiftOver (UCSC genome browser) from a previous study on a nearly identical strain [63, 64] (S2 Table). If the lifted-over transcript leaders encroached the CDS of an upstream PA14 gene, gene boundaries in the PA14 genome annotation were retained. 3' end reads within 400 nucleotides of genes were identified using the bedtools windowbed function (createFilesToAssociateWithGenes.sh). The 3' end reads and peaks were assigned to gene

transcriptional units if they satisfied either of the following conditions: a) the read is within defined operon boundaries, b) the read is downstream of the annotated 3' end of a gene and does not overlap more than 10 nucleotides into the next transcriptional unit on the same strand. The significant peaks associated with transcriptional units are identified in S3 Table (SignificantPeaksPerGeneFinder.py).

Quantifying the effects of AZM on gene expression in *P. aeruginosa*

For differential expression, we used total read counts in the 3' UTR regions of transcriptional units (all 3' reads) other than rRNAs as discussed above. The total number of reads in the 3' UTRs was compiled using a Python script that sums up the counts for reads associated with 3'UTRs of transcriptional units (DEseqFileCreateAndRunInstruction.py), and pairwise differential expression analysis of planktonic and biofilm cultures +/- AZM were performed using DEseq2 [65] (S5 and S6 Tables). Genes with an adjusted P value (pAdj) < 0.1 were considered to have significant expression differences.

Detecting relative changes in premature 3' end formation in the presence of AZM

Since transcription pausing or termination would result in reproducible peaks, we used reads corresponding to significant peaks of transcript ends in the intragenic (I) and 3'UTR regions (FL) of transcription units for protein coding genes for this analysis (IFLratioFileCreator_-Step1.py). To avoid false-positives due to low read counts, genes were only analyzed if the majority of the replicates have both I and FL read counts (no more than one zero value for I and / or FL per sample and treatment. Pseudocounts of 1 were used for all remaining zero values from I or FL peaks. Cochran-Mantel-Haenszel tests were used to identify genes with significant differences between the expected and observed read frequencies in triplicate samples of untreated and treated cultures (RcodeCMHIFL.R). The Benjamini-Hochberg procedure was used to control false discovery, with FDR < 0.1. Relative changes in levels of premature transcripts within the coding sequences of genes in response to AZM were estimated as the odds-ratio of intragenic (I) / full length (FL) 3' end peak read counts in AZM treated vs. untreated samples. Tests were performed in R (version 3.6.1) using default parameters in 2 x 2 x 3 matrices.

Predicting RNA regulatory elements in *P. aeruginosa* transcript leaders

We categorized reads present in the transcript leaders or 0–40 nucleotides into the ORF as early transcript termini reads. Percentage early termini reads (%ET) was calculated as follows:

$$\% \, ET = (\text{Early termini reads} / \text{Total 3' end reads in the gene}) * 100$$

The highest % ET that detected most predicted/known riboswitches (S11 Table) in *P. aeruginosa* was employed as a cut-off (S5A Fig) [66–68]. Genes with % ET above the cut-off in at least two replicates were considered for the next step. Since significant peaks denote 3'-ends that are reproducibly present above background noise in at least two replicates, only genes with significant peaks in their early termination zone were considered as outlier candidates. The ability of the RNA sequences upstream of significant peaks to form alternate RNA structures capable of causing Rho-independent termination were analyzed using the PASIFIC (Prediction of Alternative Structures for Identification of *cis*-regulation) web-based application [69]. Sequences were analyzed for the ability to form Rho-independent (intrinsic) terminators using ARNold [61].

Results

3pMap accurately identifies RNA 3'-OH ends

To investigate transcription-mediated regulatory mechanisms and the acute effects of AZM on the transcriptional landscape of *Pseudomonas aeruginosa*, we developed 3pMap. 3pMap adapts a commercially available RNA-seq kit to map mRNA 3' ends, by ligating a custom 3' end oligonucleotide adapter to total cellular RNA and directing library preparation to the adapter sequence (Fig 1A). Sequencing library synthesis using 3pMap has fewer steps compared to the Term-Seq approach [40] and requires minimal RNA input (2 μg) per sample.

We first applied 3pMap to *P. aeruginosa* PA14 grown under planktonic conditions in rich media in triplicate to evaluate its accuracy. We aligned the reads to the genome and identified 3' end peaks that are present in at least two replicates of a sample (significant peaks, see Methods). We assessed the distribution of 3' significant peaks in intragenic vs. intergenic regions of tRNAs and protein coding sequences (S2 Fig). Greater than 98% of significant peaks associated with tRNA genes were located within 3 nucleotides of the corresponding annotated 3' ends (S2A and S2B Fig). Similarly, 88.4% of significant peaks associated with mRNAs were located in intergenic regions, with <12% located within coding sequences (S2C Fig). These results show that 3pMap accurately detects known RNA 3' ends. We detected a small amount of ribosomal rRNAs retained in the samples after rRNA depletion. Alignment of significant peaks assigned to rRNAs confirmed the ability of 3pMap to detect RNA 3' ends accurately, and suggest alternative rRNA 3' ends that may be used in precursor or mature rRNA (S2D–S2H Fig). Together, these results illustrate that 3pMap identifies both known and novel RNA 3' ends.

Finally, we investigated the relative frequency of 3' ends in Rho-independent terminators. We used ARNOLD to predict Rho-independent terminators in the *P. aeruginosa* genome (S1 Table) [61]. ARNOLD predicts Rho-independent terminators bioinformatically using examples from *E. coli* and *B. subtilis*. On average, 18.4% of 3' end reads in significant peaks assigned to protein-coding genes overlapped predicted Rho-independent terminators (S4 Table). Since RNA 3' ends can be trimmed by nucleases [43], this represents a lower limit of the amount of 3' ends caused by Rho-independent termination. Thus, we estimate that roughly one fifth of 3' ends are generated by Rho-independent termination in *P. aeruginosa*, suggesting a substantial role for Rho-dependent termination.

The effects of AZM on *P. aeruginosa* gene expression

We next investigated how AZM alters gene expression in *P. aeruginosa*, since bacterial transcription and translation are coupled [36–39]. To understand the acute response of *P. aeruginosa* to AZM, planktonic and biofilm cultures were treated with the antibiotic for 20 minutes and 3 hours, respectively. We utilized the published transcript start sites from a nearly identical strain to define transcript leaders in the strain used in this study by converting genome coordinates with liftOver (S2 Table) [63]. To assess gene expression changes in response to AZM, we performed differential expression analysis (DEseq2) using all reads from 3' UTR regions of transcriptional units (Methods; Figs 1B, 2A and 2B, and S5 and S6 Tables) with an FDR of 10% (S7 Table). In AZM-treated planktonic cultures, 209 and 68 genes showed more than two-fold up- or down-regulation, respectively (Fig 2C). In biofilm cultures, 168 genes were downregulated and 112 genes were upregulated more than two-fold (S7 Table and Fig 2C). We observe little overlap between expression changes in planktonic and biofilm cultures, potentially due to a combination of differences in the duration of AZM treatment and lifestyle-specific gene expression patterns.

In AZM treated biofilms, we observed reduced transcript levels of several global gene expression modulators associated with stress responses (*rpoS* [70, 71], *rpoH* [72], and *relA*
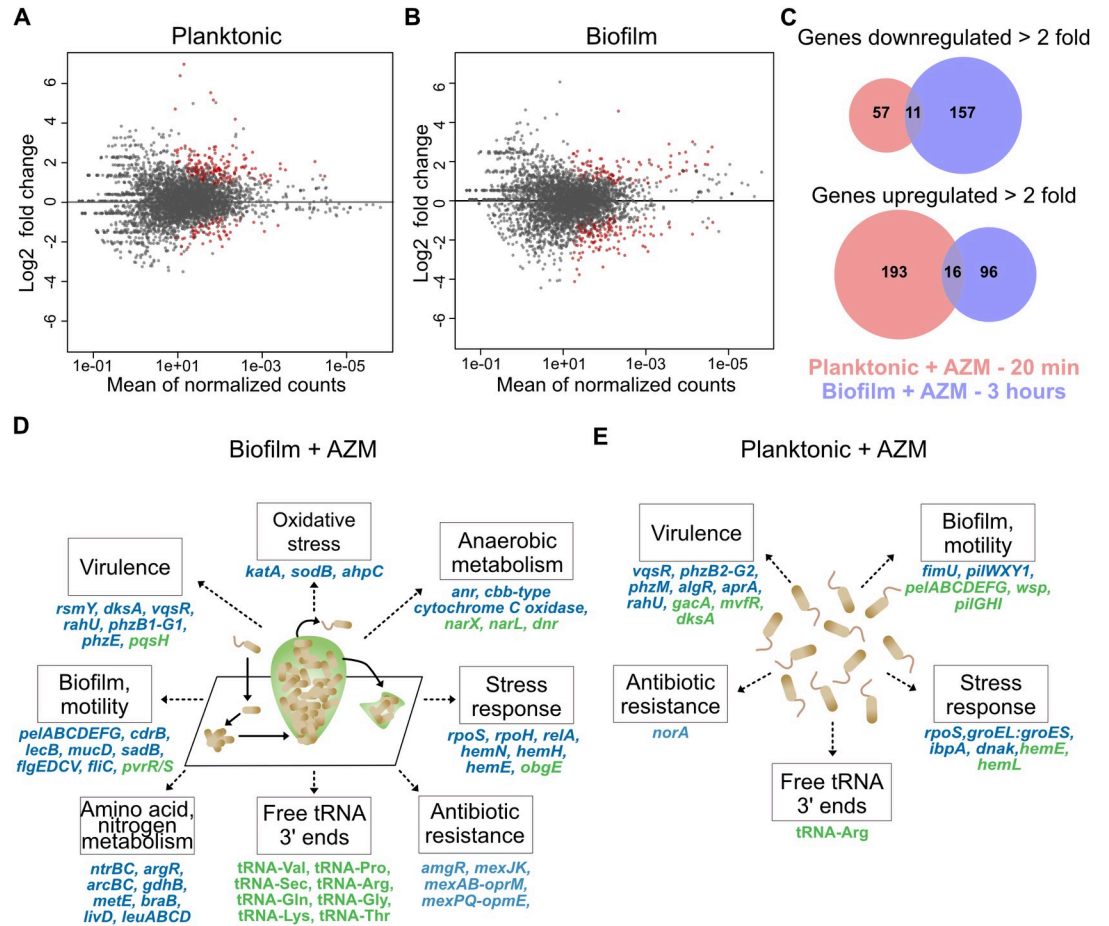
Fig 2. AZM alters full length transcript synthesis of *P. aeruginosa* genes. (A and B) Scatter plot of DEseq2 analysis of expression changes in PA14 planktonic cultures and biofilms treated with AZM. Red dots indicate DEseq changes at 10% FDR. (C) Genes showing >2 fold down (top) or up (bottom) differential regulation upon AZM treatment. AZM induced regulation of planktonic and biofilm genes, indicated in red and blue, respectively, show little overlap. Key PA14 genes regulated by AZM in biofilm (D) cultures and planktonic (E) cultures. Downregulated genes are colored blue, whereas upregulated genes are colored green. Many of these genes have pleiotropic functions, thus impact additional cell processes beyond the primary category in which they are shown here.

[73]), anaerobic metabolism (*anr* [74, 75]), virulence and biofilm formation (*rsmY* [76]), amino acid and nitrogen metabolism (*argR* [77]), *ntrBC* and *gdhB* [78]), QS (*vqsR* [79]), and antibiotic resistance *(amgR* [80]) (Fig 2D). The expression of stress, virulence, biofilm, motility, and metabolism-related genes, many of which are controlled by these regulators, were also downregulated. In contrast, AZM treatment in biofilms upregulated expression of the *obgE* GTPase (also known as CgtA) more than 20-fold. Previous work suggests that ObgE is a key player in the stringent response and promotes bacterial persistence [81, 82]. Overall, the functional categories in which multiple genes were differentially expressed here—inhibition of biofilm formation, AHL quorum sensing regulons, virulence, and stress responses—are broadly consistent with previously reported effects of AZM on *P. aeruginosa* [18, 24, 25, 28]. However, our results better define several genetic pathways that may underlie these changes, including those producing the stringent response (Fig 2D).

In planktonic cells, AZM also downregulated the expression of global gene expression modulators *rpoS* [70, 71], *vqsR* [79], and *algR* [83], and promoted early premature transcript

termini formation (S7 Table), but not significant downregulation, of *lasI*. As in biofilms, virulence factor genes were downregulated, though different genes were impacted (Fig 2E). These include phenazine biosynthesis genes *phzB2-G2* and *phzM* [84], *aprA* [85], *and rahU* [86]. Pilus genes *fimU* and *pilWXY1* were also downregulated, as were several heat shock proteins (*groEL*, *groES*, and *ibpA*, and *dnaK*) [87–90]. *mvfR (pqsR)*, a regulator of PQS quorum sensing [91], was upregulated, as was *obgE* though to a lesser extent than in biofilms (1.96-fold). In contrast to the biofilm samples, many genes associated with biofilm formation including *pelABCDEFG*, *gacA*, and the Wsp pathway were found to be upregulated upon AZM treatment, as well as haem biosynthesis proteins *hemL* and *hemE* [92–95]. The upregulation of biofilm genes is in contrast to previous studies and potentially reflects the relatively shorter duration of AZM treatment we employed or other differences in growth conditions.

We leveraged 3pMap data to evaluate differential changes in the levels of 3' OH ends associated with tRNAs in response to AZM. Charged tRNA carry cognate amino acids at their 3' ends, while uncharged tRNA have free 3' OH ends. Thus, 3pMap detects uncharged tRNAs by 3' adapter ligation to free 3' OH ends during sequencing library synthesis. We observed significantly increased levels of uncharged tRNAs upon AZM treatment—one tRNA (tRNA-Val) in planktonic, and twelve tRNAs in biofilm samples (tRNA-Arg, tRNA-Gln, tRNA-Gly,and tRNA-Lys, tRNA-Pro, tRNA-Sec, tRNA-Thr, and tRNA-Val) (S8 Table). Interestingly, the tRNA isoacceptors detected here pair with rare codons in *P. aeruginosa* (S8 Table). Whether the uncharged tRNAs detected arise from reduced tRNA aminoacylation, increased tRNA expression, or both in response to AZM remains to be characterized (see discussion).

Altered premature 3'-end formation in *P. aeruginosa* genes and operons in response to AZM

Previous work reported chronic AZM treatment impairs biofilm formation by inhibiting the expression of the *lasI/lasR* and *rhlI/rhlR* QS systems [22, 25, 27]. QS inhibition is proposed to be achieved via downregulation of the *las* and *rhl* genes [22], or downregulation of enzymes responsible for QS effector synthesis [27]. The molecular mechanisms underlying AZM-mediated regulation of QS regulators have not been determined. Although *lasI*, *lasR*, *rhlI*, and *rhlR* were not significantly downregulated in our results, we observed significant premature 3'-end peaks in *lasI* and *rhlR* upon AZM treatment (Fig 3A and 3B). We used the ratio of reads at intragenic peaks to full length peaks in 3' UTRs (I/FL) as a metric for premature 3' end formation (Fig 1B) and evaluated relative differences in I/FL in AZM-treated and untreated samples using CMH tests with a 10% FDR. To avoid false-positive results, this analysis was restricted to genes with detectable intergenic and full-length 3'-ends in both treated and control samples (Methods). AZM-treatment led to altered I/FL in 550 (63.19%) and 376 (42.1%) genes in biofilm and planktonic cultures, respectively (S9 and S10 Tables). Notably, AZM treatment resulted in extensive premature 3' end formation in the 5'-end of *lasI* and a correspondingly large increase in I/FL in biofilms (~41 fold) and in planktonic cultures (~16 fold) (Figs 3A and S3A). Similarly, an ~8 fold increase in I/FL was also observed in the *rhlR* gene in AZM treated biofilms (Fig 3B). Our results show that AZM disrupts full length *lasI* and *rhlR* expression by inducing premature 3'-end formation within their coding sequences, possibly via premature termination, transcriptional pausing or accumulation of stable nuclease products.

We next investigated whether the changes in premature intragenic 3'-end formation were pervasive feature of protein-coding genes differentially regulated by AZM (Fig 1B and S9 and S10 Tables). In biofilms, 132 differentially expressed genes had detectable intragenic and full length 3' ends in both treated and control samples, and the I/FL ratios of 111 (84.0%) of these changed significantly with AZM treatment. In planktonic cultures, I/FL measurements were
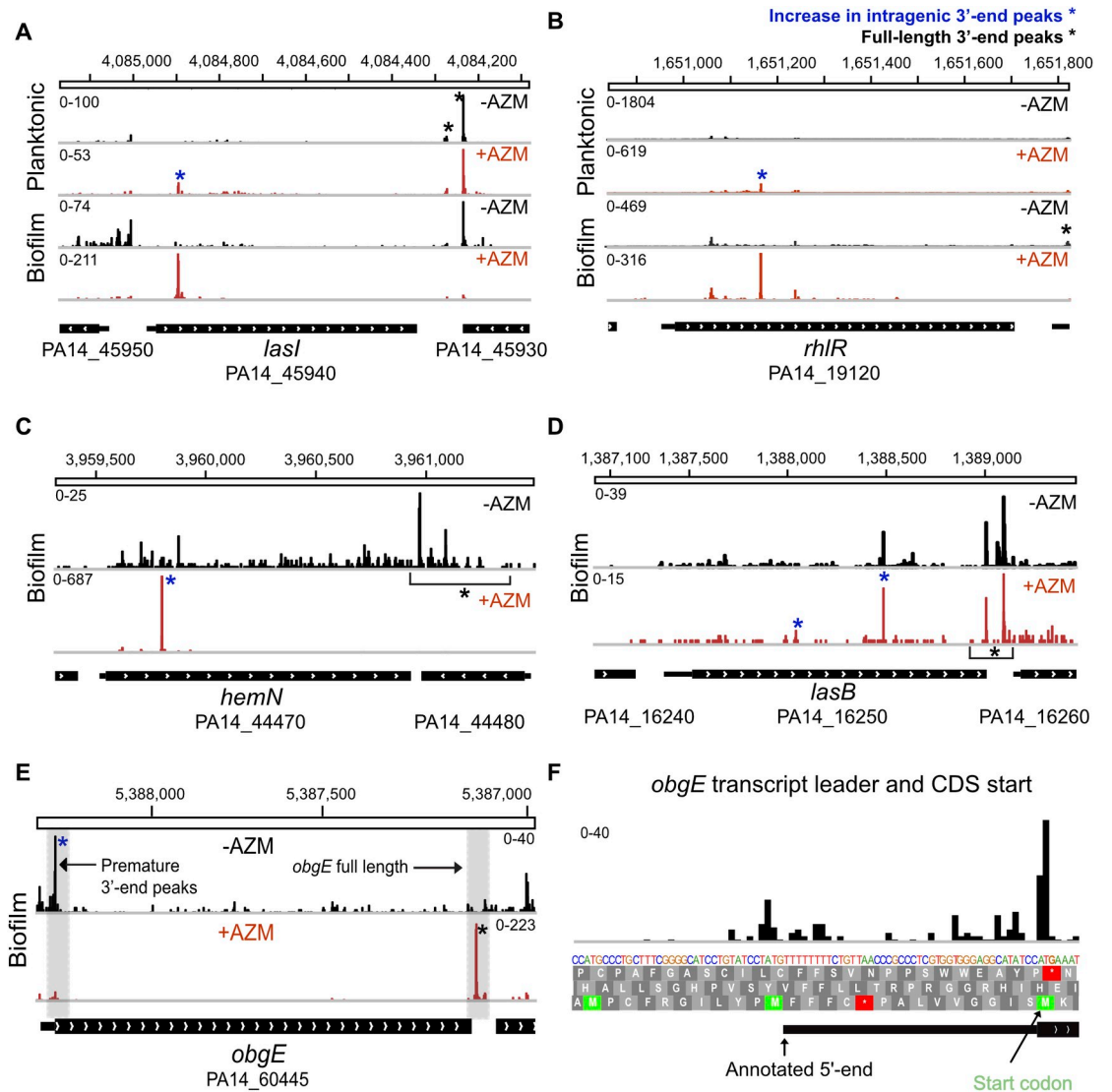
Fig 3. AZM alters intragenic 3' end peak formation in PA14 genes. (A and B) AZM dependent increase in intragenic premature 3' end peaks in *lasI* and *rhlR* genes. IGV views of *lasI* and *rhlR* in control (-AZM) and AZM treated (+AZM) treated samples from planktonic and biofilm cultures are shown. Intragenic peaks whose relative levels are altered by AZM are indicated with blue asterisks. The *lasI* gene in planktonic cultures and biofilm showed ~16 fold and ~41 fold increase in I/FL peak ratio upon AZM treatment, respectively. AZM treatment resulted in an ~8 fold increase in I/FL peaks for *rhlR* in biofilms. The peak is not prominent in planktonic cultures. **(C)** IGV view of the *hemN* gene downregulated by AZM (DEseq2 log$_2$fold change = -1.2) shows a 60 fold increase in I/FL peak ratio. The effect is less pronounced in planktonic cells **(D)** IGV view of *lasB* downregulated by AZM (DEseq2 change = ~1.95) shows moderate increase in I/FL ratio (1.74 fold) in the presence of AZM. **(E)** 23 fold upregulation of *obgE* is accompanied by a 42 fold reduction in transcription attenuation in its transcript leader. **(F)** A closer view of the transcript leader and CDS start shows termination before the rare codon for Lys at the *obgE* start codon.

https://doi.org/10.1371/journal.pgen.1009634.g003

available for 150 differentially expressed genes, and 76 (50.6%) changed with AZM treatment. Thus, compared to all genes, differentially expressed genes in biofilm and planktonic cultures were enriched ~1.3 fold and ~1.2 fold for changes in I/FL, respectively. Notably, the vast majority (93 of 100) of genes downregulated by AZM in biofilms had increased levels of premature 3' ends compared to full length transcripts (e.g Fig 3C and 3D), suggesting downregulated genes are 1.6-fold enriched for premature 3' end formation (Fisher's Exact Test (FET), p = 0.001913). These include global regulators *rpoS*, *anr*, and *relA*, as well as genes involved in

biofilm formation, stress response, and virulence factor genes such as *hemN* (Figs 3C and S3B), *lasB* (Fig 3D), *rahU* and *pelABCDEFG* [70, 71, 73, 74, 96]. The targets that exhibit no evidence of enhanced premature 3' end levels in their transcript leaders, yet are still significantly downregulated upon AZM treatment, may reflect expression changes in upstream regulators by AZM. The *lecB*, *argR*, and *sodB* genes are notable examples [25, 30, 77, 97].

Changes in premature 3' end formation could also reciprocally contribute to upregulation of genes in response to AZM treatment. Indeed, 18 of the 32 upregulated genes in biofilms, and 68 of the 118 genes upregulated in planktonic cultures exhibited corresponding decreases in premature intragenic 3' end formation, an 8.1-fold enrichment in biofilms and a 2.6-fold enrichment in planktonic cultures (FET p < 7.8 x 10^{-8}). The most upregulated gene in AZM-treated biofilms is *obgE*, a conserved GTPase involved in the stringent response and persistence in *P. aeruginosa* [81, 82]. Notably, *obgE* also showed the highest reduction in I/FL peak ratio in response to AZM through a striking reduction in premature 3' end formation at the ObgE start codon (Figs 3E, 3F and S4). Thus, relief of premature 3' end formation occurs at most genes upregulated by AZM and may contribute to induction of the stringent response. These data suggest that premature 3' end formation contributes to the gene expression response to AZM, such that increased premature 3' end formation downregulates the expression of some genes, while decreased premature 3' end formation upregulates the expression of others.

Predicting RNA regulatory elements that in *P. aeruginosa* transcript leaders

Transcription regulation by attenuators, riboswitches, RNA thermometers, sRNAs etc. can result in premature 3' ends in the transcript leaders and surrounding sequences [46–49, 98]. We reasoned that transcript leaders regulated by early transcription termination, pausing, and / or targeted degradation would be characterized by a high incidence of 3' end formation detectable by 3pMap. To identify genes with high incidence of premature transcript termini in their early termination zone (transcript leader + 40 nucleotides in the coding sequence) (Fig 1C and Methods), we calculated the percentage early termini (% ET) for each gene in planktonic and biofilm samples grown +/- AZM. The median %ET was < 3.0% for the tested samples (Figs 1C and S5B). As riboswitch activity has been shown to result in reproducible premature 3'-end termini, we used a heuristic cut-off of 30%, which is >10-fold above the median %ET and sufficient to detect most riboswitches documented on Rfam and predicted by Riboswitch Scanner to predict genes with regulatory mechanisms causing premature 3'-termini formation in their early termination zone (S5A Fig and S11 Table) [66–68]. Genes with %ET values <30% and lacking significant peaks representative of reproducible 3' end termini in the transcript leaders were not considered in further analysis (e.g. Fig 4A).

We identified 282 protein-coding genes with more than 30% of their 3' ends in the early termination zone (S12 Table). This included genes previously reported to be controlled by transcription termination in *P. aeruginosa* or other bacteria, e.g. *amiE* operon (Figs 4B and S5C–S5F), attesting to the ability of our approach to predict genes that are potentially regulated in this manner [99–102]. The gene with highest early transcription termination is *rhlI*, from whose transcript leader the sRNA *rhlS* was recently reported to be derived [103] (S5C Fig). We further utilized PASIFIC, a bioinformatic tool for predicting regulation via alternate structure formation and rho-independent termination to examine our new candidates for potential alternate structure formation and regulation by premature transcription termination [69], and ARNOLD [61] to separately predict rho-independent terminators (S13 Table). Forty-one premature termination candidate genes were predicted to have the propensity to form alternate
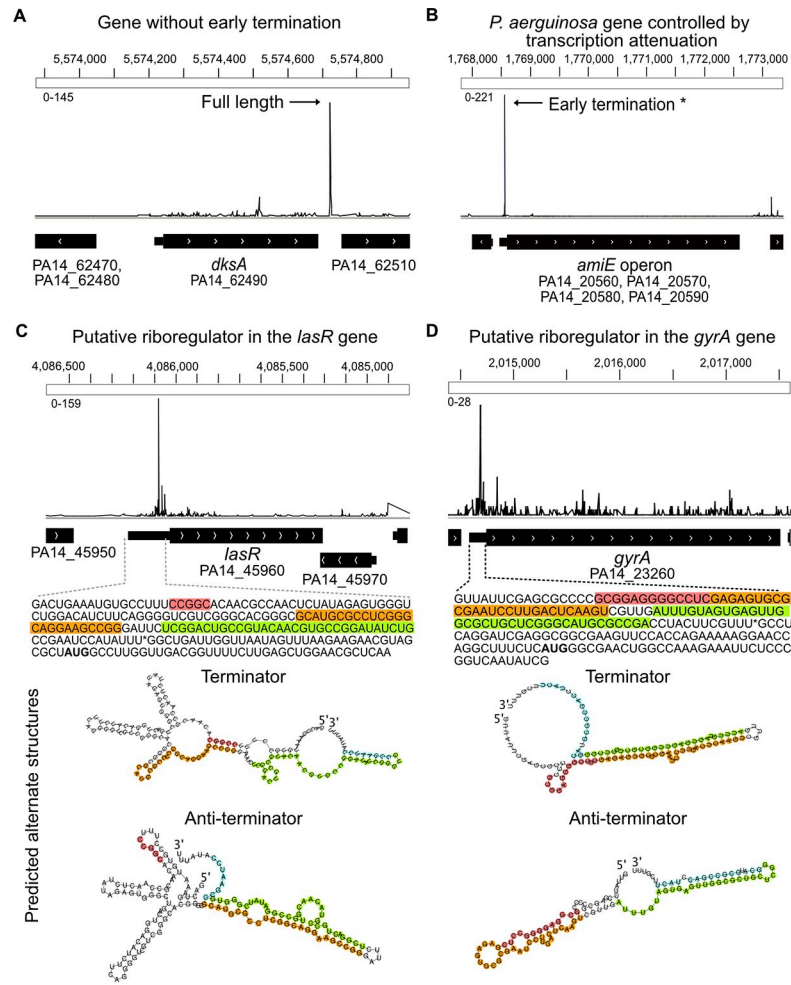
Fig 4. Predicting genes regulated by premature 3' end formation in transcript leaders. IGV views show strand-specific 3' end counts. (A) Example of a gene (*dksA* PA14_62490) not predicted to be regulated by premature transcription termination in its transcript leader. The major 3' end peak is in the 3' UTR. (B) IGV view of early termination in the *amiE* operon, known to be regulated by transcription attenuation, shows major 3' end peak in transcript leader. (C) IGV view of *lasR* shows premature 3' end peaks in its transcript leader. The sequence of the *lasR* early termination region and predicted alternate secondary structures in the transcript leader are shown below. The asterisk denotes a premature 3' end peak. Alternate structures with potential to effect early termination (terminator and transcriptional read-through (anti-terminator was predicted with PASIFIC [68] using the sequence upstream of the asterisk (corresponding to a 3' end significant peak) as the input. (D) IGV view of DNA gyrase A (*gyrA*) shows premature 3' ends in its transcript leader. The sequence of *gyrA* transcript leader and 40 nt in the CDS and the alternate structures predicted by PASIFIC are shown below, as in C.

structures and / or contain rho-independent terminators. Notably, these new candidates included several genes critical for *Pseudomonas* biology, such as the QS and virulence gene *lasR* [104] (Fig 4C), DNA gyrase A (*gyrA*)—associated with fluoroquinolone-resistance currently being explored as a pharmacological target (Fig 4D) [105–107], and the cytochrome c oxidase operon (not shown). Further biochemical and functional analysis of these candidate regulatory elements could provide insights into mechanisms controlling *P. aeruginosa* gene expression. In summary, we identify hundreds of genes in *P. aeruginosa* putatively regulated by early transcription termination or nuclease action, many of which were predicted to form alternate structures.

Discussion

In this study, we used 3pMap to identify RNA 3' ends in *P. aeruginosa* and to gain insights into gene regulation in response to AZM. Our study provides new insights into the role of transcriptional regulation in the *P. aeruginosa* response to AZM. Most downregulated genes, including many key transcriptional regulators and their targets—exhibit enhanced premature 3' end formation. We also found reduced transcription attenuation in some upregulated genes upon AZM treatment, most notably inducing expression of *obgE*, a central component of the stringent response. Finally, we identified over two hundred genes exhibiting high levels of premature transcript termini in or near their 5' transcript leaders. The sequences surrounding many of the premature transcript termini are predicted to form alternate structures and/or rho-independent terminators, suggesting some may be controlled by riboregulation (S13 Table). The implications of these results for understanding *P. aeruginosa* biology and therapeutic interventions are discussed below.

Chronic *P. aeruginosa* infections are common in CF patients, and sub-inhibitory concentrations of AZM improve clinical outcomes [13–15]. AZM impairs biofilm formation due to altered expression of QS and virulence genes [21–29]. Previous work proposed the effects of AZM on QS resulted from inhibition of the synthesis of specific proteins [22, 27]. First, AZM might disrupt the translation of an unknown protein which in turn controls the transcription of autoinducer synthases *lasI and rhlI* [22]. Secondly, AZM might downregulate the expression of N-acyl homoserine lactone (AHL) synthesis enzymes upstream of *lasI* and *rhlI*, which in turn further dampen AHL production and inhibit QS [27]. However, because the assays used in these previous studies did not differentiate between full-length and truncated transcripts, neither of the resulting models consider the impact of AZM-induced translational stalling on coupled mRNA transcription. We investigated the role of transcription regulation on the *P. aeruginosa* response to AZM using 3pMap. AZM greatly elevated the levels of premature transcripts in primary QS regulators *lasI* (in planktonic and biofilm cultures) and *rhlR* (in biofilms) (Fig 3A and 3B). Thus, our results suggest AZM directly impacts expression of QS genes by regulating transcription or transcript stability.

Importantly, we found AZM induced premature transcript formation in key transcriptional regulators of biofilm formation and virulence (S7 Table). Such increases in premature transcript formation accompanied the downregulation of *rpoS*, *rpoH*, *vqsR* and *anr* [70–72, 74, 75, 79]. *Anr* regulates QS and virulence gene expression in low-oxygen environments such as biofilms [74, 75]. In QS mutants isolated from infections, *anr* plays a compensatory role in virulence gene expression. The expression of *rpoS*, an alternative sigma factor and a master regulator of *P. aeruginosa* stress response [70, 71] was downregulated by AZM in planktonic cells as well. Increased premature 3' end formation also accompanied downregulation of virulence factor genes targeted by QS (*lasB*, *phzB-G*, *pelABCD*, *rahU*) [25, 85, 86, 108]. The premature 3'-ends we discovered could result from altered premature termination, transcription pausing, or from nuclease activities. Taken together, our results support a model in which AZM-induced premature 3' end formation reduces the expression of these central transcriptional modulators (Fig 5A).

The effects of AZM on *P. aeruginosa* gene expression are reminiscent of previous work in other bacteria, which showed ribosome-acting antibiotics can alter target gene transcription by stalling translation [36, 109–112]. In *E. coli*, slowing translation with sublethal concentrations of chloramphenicol uncouples transcription from translation, thereby slowing transcription elongation rates and/or triggering premature transcription termination [37, 112]. Macrolide-mediated ribosome stalling is not uniformly distributed across genes but instead is determined by specific sequence features of nascent polypeptides [113]. In *Staphylococcus*
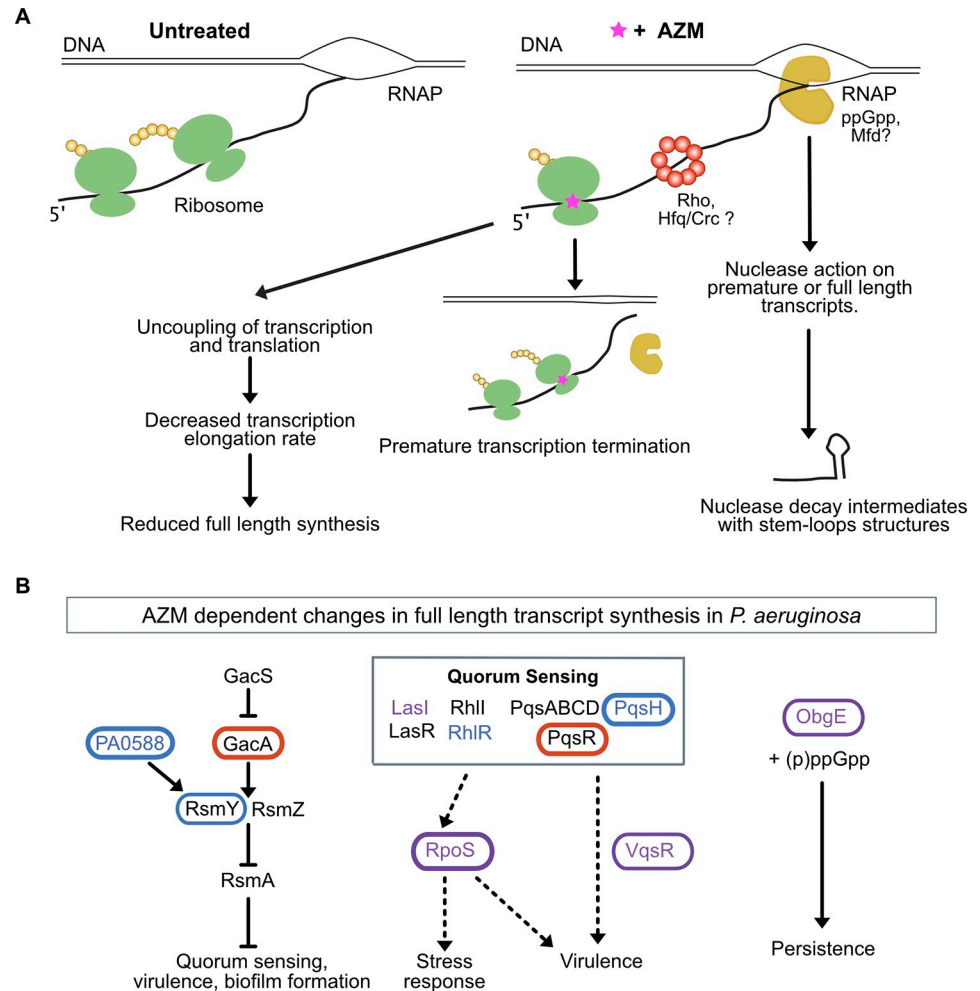
Fig 5. Model of *P. aeruginosa* response to azithromycin. (A) Altered premature 3'-end formation is observed in up and down-regulated genes/operons of *P. aeruginosa* in response to AZM. AZM induces changes in premature transcription termination, transcription pausing and/or transcription elongation rate, due to transcription-translation uncoupling or altered RNA polymerase pausing in response to ppGpp, thereby resulting in gene expression changes. Alternatively, nuclease action on premature and full-length transcripts could contribute to gene expression changes in response to AZM. Different molecular mediators of transcriptional control that could affect transcriptional changes are indicated–Rho and Mfd (transcription termination), ppGpp (RNAP pausing), and Hfq (sRNA action and nuclease recruitment). **(B)** Impact of AZM on gene expression of key *P. aeruginosa* regulators. Network diagram depicts several genes found to be differentially regulated and exhibit premature transcription termination within the GacS/GacA signal transduction system, quorum sensing systems, and stringent response regulators. These genes, and their regulons, have been shown to be highly interconnected, therefore only a subsection of interactions are shown here. Oval outlines indicate that a gene was differentially expressed upon AZM treatment as detected by DESeq2. Significant hits for altered relative I/FL ratio upon AZM treatment is shown by color of the text. Genes with altered expression or early transcription termination in biofilms are indicated in blue, in planktonic culture in red, and in both conditions in purple. The nature of the expression changes is indicated in Fig 3D.

aureus, AZM caused sequence-specific ribosome stalling in the middle or late stages of translation [32, 33]. Interestingly, AZM-specific ribosome stalling hotspots, referred to as 'macrolide arrest motifs' [114], were enriched in virulence-related and essential genes [113]. By quantifying premature transcription, we found premature transcript termini accumulate at most, if not all, downregulated genes in *P. aeruginosa*. This accumulation of premature transcripts likely reflects sequence-specific ribosome stalling. One interesting possibility is that *P. aeruginosa* has evolved macrolide-responsive stall sequences in QS and stress response genes (e.g. *rpoS*

and *lasI*) to promote survival in response to macrolides produced by environmental competitors [115]. Additional studies, including ribosome profiling, are needed to identify translation stalling motifs in *P. aeruginosa* and further investigate antibiotic induced ribosome stalling on transcription.

Bacterial transcription termination occurs via intrinsic and factor-dependent mechanisms mediated by Rho and Mfd [44, 45]. Other work has shown that sRNAs can antagonize Rho-dependent termination, e.g. at the *E. coli rpoS* gene [116]. We find that roughly one-fifth of reads in significant 3' end peaks correspond to predicted rho-independent or intrinsic terminators, suggesting most termination in *P. aeruginosa* is factor-dependent (S3 Table). AZM treatment did not considerably change the proportion of reads in peaks overlapping intrinsic terminators in biofilms and planktonic cultures, suggesting that factor-dependent termination could play an important role in *P. aeruginosa* AZM response.

It is possible that some of the altered 3'-end significant peaks observed in AZM-treated samples could be nuclease-degradation intermediates with stable structures. In bacteria, ribosome occupancy and events occurring during translation influence the susceptibility of mRNAs to ribonuclease attack [117]. Transcriptional pausing and translation-transcription uncoupling are thought to increase endonucleolytic RNase cleavage [117–119]. The cleavage products are quickly acted upon by 3' exonucleases until they encounter thermodynamically stable stem-loop structures. Consequently, the possibility of increased nuclease action on some mature and nascent transcripts in AZM-treated samples cannot be ruled out. For example, *hemN* and *rpoS* have been reported to be bound by *Hfq* in *P. aeruginosa* strain PA01 in the absence of antibiotics [120]. However, we also note that low levels of antibiotics that inhibit translation have been found to stabilize mRNAs typically associated with drug resistance in Gram-positive bacteria (e.g. *S. aureus* and *B.subtilis ermA* and *ermC* [121, 122]).

An interesting observation from our study is the differential increase in tRNA 3'-end levels in response to AZM.The increased 3'-ends for tRNAs, particularly rare codon tRNAs for Arg, Lys, Pro, Gln, Gly, Sec, and Val in biofilms (S7 Table), could arise from reduced aminoacylation or an increase in tRNA gene expression. Reduced aminoacylation could cause translational stalling at rare codons, further altering the synthesis of full-length transcripts (Fig 5A) [110, 111]. Increased tRNA gene expression, unless accompanied by proportionate increases in aminoacylation, could dilute the pool of charged tRNA. In this case, the net effect would also be increased translational stalling at these rare codons. The influence of rare codons on translation and transcription elongation rates is well documented in *E. coli* [107], and tRNA concentrations and codon decoding times are positively correlated in many prokaryotes [13, 116]. Interestingly, replacing a rare codon (AGG, frequency = 0.6 / 1000) for Arginine at the second codon position of the QS gene *rhlR* with the most frequently used codon (CGC, frequency = 48.8 / 1000) was previously shown to alleviate the inhibitory effects of AZM on virulence factor production in *P. aeruginosa* [123]. Our results suggest tRNAs targeting rare codons for Arg, Lys, Pro, Gln, Gly, Sec, and Val were more often uncharged after AZM treatment in biofilms. This decrease in tRNA charging could cause ribosome stalling at rare codons, altering the synthesis of full-length transcripts. Deacylated/uncharged tRNAs bind to the A-site on the ribosome, eventually triggering stringent response mechanism [124]. The stringent response leads to elevated levels alarmones such as ppGpp and ppppGpp, which are known to regulate RNA polymerase and help bacteria to survive under adverse conditions. Future work evaluating the role of tRNAs in the *P. aeruginosa* response to AZM would be beneficial.

AZM treatment caused upregulation of *obgE*, a conserved GTPase that binds ppGpp and mediates the stringent response and persistence under various stresses by increasing the dissociation of stalled 70S ribosomal units [82, 83, 125]. 3pMap identified a prominent 3' end

significant peak in the first codon of the *obgE* ORF (Fig 3E and 3F). AZM-induced upregulation of *obgE* coincided with significantly reduced levels of premature 3' end termini in the transcript leader, suggesting it may be regulated by a transcriptional attenuator. Ribosome stalling on upstream open reading frames (uORFs) in transcript leaders have been shown to relieve premature transcription termination of response to the macrolide lincomycin in *L. monocytogenes* [40]. Curiously, the *obgE* transcript leader contains a uORF (Figs 3F and S4), which may play a similar role in upregulating full-length transcription through attenuation. However, this attenuation-by-uORF mechanism seems insufficient because the observed premature termination occurs at the *obgE* start codon, which is followed by a rare codon for lysine, not in an intrinsic terminator. This suggests additional regulatory factors may contribute to the switch to full length transcription in the presence of azithromycin. For example, the switch to full length transcription may be independent of the uORF, instead relying on Rho, other *trans*-acting factors or uncharged tRNA. Notably, transcriptional pausing often occurs at translation start sites in *E. coli* and *B. subtilis*[126], and ppGpp has been shown to bind directly to *E. coli* RNA polymerase and alter its pausing behavior [127], which could potentially relieve premature termination in *obgE*. Future work is needed to determine the mechanisms underlying transcriptional regulation of *obgE*.

RNA-based regulatory strategies are gaining traction as antibacterial therapeutic targets [13, 52, 128, 129]. For example, the FMN riboswitch controls expression of flavin mononucleotide synthesis operons in many bacteria. Ribocil, a small molecule that targets the riboswitch by mimicking the FMN ligand, reduced bacterial growth of *E. coli* in a mouse systemic infection model [128]. Similarly, a small molecule targeting the guanine riboswitch, PC1, inhibited growth of *S. aureus* in mouse and cow infection models [129, 130]. The candidates we identified provide a first transcriptome-wide catalogue of candidate genes regulated via mechanisms targeting transcript leaders such as premature transcription termination, translation inhibition, or nuclease action in *P. aeruginosa*, which have the potential to inform experimental studies to discover 'druggable RNAs'. However, due to the compact nature of bacterial genomes, some of the candidate riboregulators may represent termination sites from upstream genes. On the other hand, many riboswitches and attenuators may still await discovery, as these elements are condition-specific and may require interactions with the host immune system or other cellular stresses for their activity. Indeed, our heuristic 30% ET threshold may miss elements that were less active in the metabolic conditions of the media used in our study. Additionally, some could produce novel sRNAs with regulatory roles, as was recently reported for *rhlI* [103]. Thus, further studies are needed to probe the transcriptional regulation of the elements identified here and to identify the full set of bona fide riboregulators in *P. aeruginosa*.

Regardless of the molecular mechanisms utilized, our results reveal that the accumulation of alternative 3' termini is a hallmark of the response to AZM by *P. aeruginosa* that may contribute to changes in QS and virulence gene expression. We propose a model in which the AZM-induced premature transcription termination, pausing, and/or nuclease action on multiple central transcriptional modulators cascades through their regulatory targets (Fig 5B). Furthermore, the AZM-dependent increase in tRNA 3'-ends and induction of *obgE* expression suggest that AZM may trigger the stringent response and persistence in *P. aeruginosa*. This implies that the efficacy of AZM as an anti-virulence treatment may trade off against the induction of persister phenotypes, a phenomenon warranting further study. In summary, we provide new insights into how AZM treatment affects the transcriptional landscape of *P. aeruginosa*, which has important implications for the development and implementation of treatments for infections.

Supporting information

S1 Fig. The Minimum Inhibitory Concentration (MIC) of AZM was determined by broth microdilution according to CLSI guidelines [131]. Three replicate assays were performed. Briefly, twofold microdilutions of Azithromycin dihydrate (Fisher J66740) in Mueller Hinton Broth were inoculated with $5x10^5$ CFU/mL PA14 in a 96 well plate. After 16–20 hours of incubation at 37˚C, MIC was determined to be the lowest concentration of antibiotic at which no visible growth was observed.
(TIFF)

S2 Fig. Genome-wide mapping of RNA 3' ends in untreated planktonic cultures of PA14 using 3pMap. (A). Location of 3pMap reads with respect to the 3' end of tRNAs (RNA end = 0 nucleotide). 98.78% of the significant peaks within or downstream of tRNAs are located within 3 nucleotides from the annotated RNA ends. **(B)** Genome browser view of distribution of 3' ends around two tRNA genes. Number of 3' end reads corresponding to each sample are denoted on the top of the sample tracks. **(C)** Location of 3pMap reads with respect to the 3' end of CDSs. RNA 3' end = 0 nucleotide. 88.4% of significant peaks associated with mRNAs were located in intergenic regions, with <12% located within coding sequences. **(D)** Location of 3pMap reads with respect to the 3' end of 23S ribosomal RNAs. 99.8% of the significant peaks within or downstream of 23SrRNA genes are located within 3 nucleotides of the annotated RNA ends. **(E)** Genome browser view of the distribution of 3' ends around representative 23S rRNA and 5S rRNA genes. **(F)** Extended 16S rRNAs in *Pseudomonas aeruginosa*. 80.54% of the detected 16S rRNAs (<10,000 reads in three replicates) had RNA 3' ends in +35 and +36 nucleotides downstream of their annotated RNA 3' ends. A recent study reported extended anti-Shine Dalgarno motifs in 16S rRNA in other bacteria, although they failed to identify such a motif in *P. aeruginosa* [132]. The major peak +35/36 downstream of 16S rRNA could represent extended anti-Shine Dalgarno motifs in *P. aeruginosa* 16S rRNA, capable of providing additional specificity or transcript preference for Shine Dalgarno motifs on mRNA, or unprocessed pre-16S rRNAs [132, 133]. **(G)** 99.9% of RNA 3' end significant peaks associated with 5S rRNAs were located -8 or -7 nucleotides upstream of their annotated RNA ends. **(H)** Alignment of 5S rRNA sequences from PA01 and PA14 genome annotations using Clustal Omega (www.ebi.ac.uk). The prokaryotic 5S rRNA sequence is well conserved and 120 nucleotides long, including in the PAO1 strain (Pseudomonas genome database). We aligned the 5S rRNA sequences from PAO1 and our PA14 using Clustal Omega (www.ebi.ac.uk), and found that the 3' end identified by 3pMap is identical to PAO1. The 3' end identified by 3pMap matches with the annotated PA01 5S rRNA 3' end.
(TIFF)

S3 Fig. Changes in intragenic to full-length transcript ratios of *lasI* and *hemN*. Total RNA was phenol-chloroform extracted from biofilm samples and treated with 1 unit of RQ1 RNase-Free DNase (Promega M6101) according to manufacturer's protocol to remove any residual genomic DNA. DNase-treated RNA was reverse transcribed using a 2 μM pooled mixture of reverse primers for the target genes of interest (S14 Table) and Superscript IV Reverse Transcriptase (Thermofisher Scientific 18090010). The reverse transcription reaction for intragenic and full-length transcripts were performed for 20 minutes at 55˚C. cDNA was amplified with the corresponding primer pairs (S14 Table) for targets of interest and Sybr Green PowerUp Master Mix (Thermofisher Scientific A25741) according to the manufacturer's protocol on Applied Biosystems StepOne Plus Real-Time PCR system. For each condition, three biological replicates were tested, with three technical replicates for each.
(TIFF)

S4 Fig. Full coverage strand-specific 3pMap reads for *obgE* transcript leader. Tracks for all three replicates of biofilm treated (AZM) and untreated (U) samples are shown. The numbers on the scale depict original, non-normalized read counts. Both AUG methionines of the potential uORF, though outside the annotated transcript leader from Wurtzel *et al.*, are covered by transcribed RNA in vivo. Note the strong accumulation of 3' ends at the *obgE* start codon, which appears as a "cliff" before coverage drops (compare to Fig 3).
(TIFF)

S5 Fig. Early termination in PA14 transcript leaders. (A) Determining the early termination zone. Number of known riboswitches reported on Rfam detected for each ET zone and %ET cut off considerations. The lowest ET zone consideration of transcript leader + 40 nt in CDS and the highest cut-off value of 30% detected 8/11 riboswitches reported on Rfam, and was therefore used for predicting putative riboregulators. **(B)** Box Whisker plot showing the distribution of %ET values in samples using ET zone transcript leader + 40 nt of CDS. **(C)** Early transcription termination in the *rhlI* gene detected by 3pMap [133]. Genome browser images show strand-specific tracks for the strand same as the gene of interest and in untreated planktonic samples unless specified. **(D)** Potential regulation of the *pyRG* gene by in *P. aeruginosa* by 3' end formation in its transcript leader. The *pyrG* expression is controlled by transcription attenuation in *B. subtilis* [134]. Genome browser image shows *pyrG*, *kdsA* operon. **(E)** Premature 3' end formation in *trpGDC* operon in *P. aeruginosa* biofilms. %ET values in planktonic (untreated and +AZM) and untreated biofilm samples were below the cut-off value. However, in AZM-treated biofilms (+AZM), regulation by premature 3' end formation was predicted. The gene is predicted to be regulated by transcription attenuation in *B. subtilis* [135]. **(F)** A closer view of the transcript leader and early termination peak in *trpGDC* operon. The 3' end peaks are located adjacent to a potential uORF with GTG start codon.
(TIFF)

S1 Table. Genomic coordinates of Rho-independent terminators in *P. aeruginosa* genome predicted using ARNold webserver.
(XLSX)

S2 Table. Genomic coordinates of genes and operons written similar to bed format and used for bedtools and assigning 3'-end reads and peaks to transcript leaders, intragenic or operon, and 3pUTR categories.
(XLSX)

S3 Table. 3' end significant peaks associated with genes and operons in *P. aeruginosa*.
(XLSX)

S4 Table. Percentage of 3' end significant peaks associated with rho-independent terminators in the protein coding genes.
(XLSX)

S5 Table. Read counts associated with 3' UTRs of genes/operons replicates in untreated (U) and azithromyin-treated (AZ) biofilm(BF) samples and differential expression analysis results from DEseq2.
(XLSX)

S6 Table. Read counts associated with 3' UTRs of genes/operons replicates in untreated (U) and azithromyin-treated (AZ) biofilm(BF) samples and differential expression analysis results from DEseq2.
(XLSX)

S7 Table. DEseq2 results—Log2fold changes with pAdj < 0.1 in biofilm (BF) and planktonic (Pl) samples. NS denotes "not significant" and represents log2 fold changes with pAdj value > 0.1.
(XLSX)

S8 Table. tRNA genes with greater than two-fold change in 3' end reads up on AZM treatment.
(XLSX)

S9 Table. Relative changes in the ratio of reads in internal peaks (I) to reads in Full length peaks (FL) in planktonic samples.
(XLSX)

S10 Table. Relative changes in the ratio of reads in internal peaks (I) to reads in Full length peaks (FL) in biofilm samples.
(XLSX)

S11 Table. Rfam annotated riboregulatory elements in *P. aeruginosa* (PA01).
(XLSX)

S12 Table. Percent Early Termini reads (%ET) for all protein coding genes/operons in *P. aeruginosa*.
(XLSX)

S13 Table. Genes predicted to form alternate structures by PASIFIC or Rho-independent transcription terminators predicted by ARNold in their ET zone.
(XLSX)

S14 Table. Primers used for RT-qPCR.
(XLSX)

S1 Scripts. This file contains all of the custom scripts used for data analysis as cited in the methods section of the manuscript.
(ZIP)

Acknowledgments

Author Contributions

Conceptualization: Salini Konikkat, N. Luisa Hiller, Vaughn S. Cooper, Joel McManus.

Data curation: Salini Konikkat.

Formal analysis: Salini Konikkat, Joel McManus.

Funding acquisition: Vaughn S. Cooper, Joel McManus.

Investigation: Salini Konikkat, Michelle R. Scribner, Rory Eutsey.

Methodology: Salini Konikkat, Rory Eutsey.

Project administration: Vaughn S. Cooper, Joel McManus.

Software: Salini Konikkat, Joel McManus.

Supervision: N. Luisa Hiller, Vaughn S. Cooper, Joel McManus.

Visualization: Salini Konikkat, Michelle R. Scribner.

Writing – original draft: Salini Konikkat, Joel McManus.

Writing – review & editing: Salini Konikkat, Michelle R. Scribner, N. Luisa Hiller, Vaughn S. Cooper, Joel McManus.

References

1. Peleg AY, Hooper DC. Hospital-acquired infections due to Gram-negative bacteria. N Engl J Med. 2010; 362: 1804–1813. https://doi.org/10.1056/NEJMra0904124 PMID: 20463340

2. Driscoll JA, Brody SL, Kollef MH. The epidemiology, pathogenesis and treatment of *Pseudomonas aeruginosa* infections. Drugs. 2007; 67: 351–368. https://doi.org/10.2165/00003495-200767030-00003 PMID: 17335295

3. Gellatly SL, Hancock RE. *Pseudomonas aeruginosa*: new insights into pathogenesis and host defenses. Pathogens Disease. 2013; 67: 159–173. https://doi.org/10.1111/2049-632X.12033 PMID: 23620179

4. Ramirez Estrada S, Borgatta B, Rello J. *Pseudomonas aeruginosa* ventilator-associated pneumonia management. Infect Drug Resist. 2016; 9: 7–18. https://doi.org/10.2147/IDR.S50669 PMID: 26855594

5. Wu DC, Chan WW, Metelitsa AI, Fiorillo L, Lin AN. *Pseudomonas* skin infection: clinical features, epidemiology, and management. Am J Clin Dermatol. 2011; 12: 157–169. https://doi.org/10.2165/11539770-000000000-00000 PMID: 21469761

6. Markou P, Apidianakis Y. Pathogenesis of intestinal *Pseudomonas aeruginosa* infection in patients with cancer. Front Cell Infect Microbiol. 2014; 3: 115. https://doi.org/10.3389/fcimb.2013.00115 PMID: 24432250

7. Wagner VE, Iglewski BH. *P. aeruginosa* biofilms in CF Infection. Clin Rev Allergy Immunol. 2008; 35: 124–134. https://doi.org/10.1007/s12016-008-8079-9 PMID: 18509765

8. Jolivet-Gougeon A, Bonnaure-Mallet M. Biofilms as a mechanism of bacterial resistance. Drug Discov Today Technol. 2014; 11: 49–56. https://doi.org/10.1016/j.ddtec.2014.02.003 PMID: 24847653

9. Wei Q, Ma LZ. Biofilm matrix and its regulation in *Pseudomonas aeruginosa*. Int J Mol Sci. 2013; 14: 20983–21005. https://doi.org/10.3390/ijms141020983 PMID: 24145749

10. Bjarnsholt T. The role of bacterial biofilms in chronic infections. APMIS Supplementum 2013;: 1–51. https://doi.org/10.1111/apm.12099 PMID: 23635385

11. Mulcahy LR, Isabella VM, Lewis K. *Pseudomonas aeruginosa* biofilms in disease. Microb Ecol. 2014; 68: 1–12. https://doi.org/10.1007/s00248-013-0297-x PMID: 24096885

12. Høiby N, Krogh Johansen H, Moser C, Song Z, Ciofu O, Kharazmi A. *Pseudomonas aeruginosa* and the *in vitro* and *in vivo* biofilm mode of growth. Microbes Infect. 2001; 3: 23–35. https://doi.org/10.1016/s1286-4579(00)01349-6 PMID: 11226851

13. Howe RA, Spencer RC. Macrolides for the treatment of *Pseudomonas aeruginosa* infections? J Antimicrob Chemother. 1997; 40: 153–155. https://doi.org/10.1093/jac/40.2.153 PMID: 9301978

14. Schultz MJ. Macrolide activities beyond their antimicrobial effects: macrolides in diffuse panbronchiolitis and cystic fibrosis. J Antimicrob Chemother. 2004; 54: 21–28. https://doi.org/10.1093/jac/dkh309 PMID: 15190022

15. Blasi F, Bonardi D, Aliberti S, Tarsia P, Confalonieri M, Amir O, et al. Long-term azithromycin use in patients with chronic obstructive pulmonary disease and tracheostomy. Pulm Pharmacol Ther. 2010; 23: 200–207. https://doi.org/10.1016/j.pupt.2009.12.002 PMID: 20025989

16. Yousef AA, Jaffe A. The role of azithromycin in patients with cystic fibrosis. Paediatr Respir Rev. 2010; 11: 108–114. https://doi.org/10.1016/j.prrv.2009.12.003 PMID: 20416547

17. Taylor SP, Sellers E, Taylor BT. Azithromycin for the prevention of COPD exacerbations: The good, bad, and ugly. Am J Med. 2015; 128: 1362.e1–6. https://doi.org/10.1016/j.amjmed.2015.07.032 PMID: 26291905

18. Hoffmann N, Lee B, Hentzer M, Rasmussen TB, Song Z, Johansen HK, et al. Azithromycin blocks quorum sensing and alginate polymer formation and increases the sensitivity to serum and stationary-growth-phase killing of *Pseudomonas aeruginosa* and attenuates chronic *P. aeruginosa* lung infection in Cftr(-/-) mice. Antimicrob Agents Chemother. 2007; 51: 3677–3687. https://doi.org/10.1128/AAC.01011-06 PMID: 17620382

19. Stellari F, Bergamini G, Sandri A, Donofrio G, Sorio C, Ruscitti F, et al. In vivo imaging of the lung inflammatory response to *Pseudomonas aeruginosa* and its modulation by azithromycin. J Transl Med. 2015; 13: 251–10. https://doi.org/10.1186/s12967-015-0615-9 PMID: 26239109

20. Molinari G, Paglia P, Schito GC. Inhibition of motility of *Pseudomonas aeruginosa* and *Proteus mirabilis* by subinhibitory concentrations of azithromycin. Eur J Clin Microbiol Infect Dis. 1992; 11: 469–471. https://doi.org/10.1007/BF01961867 PMID: 1330564

21. Molinari G, Guzmán CA, Pesce A, Schito GC. Inhibition of *Pseudomonas aeruginosa* virulence factors by subinhibitory concentrations of azithromycin and other macrolide antibiotics. J Antimicrob Chemother. 1993; 31: 681–688. https://doi.org/10.1093/jac/31.5.681 PMID: 8392997

22. Tateda K, Comte R, Pechere JC, Köhler T, Yamaguchi K, Van Delden C. Azithromycin inhibits quorum sensing in *Pseudomonas aeruginosa*. Antimicrob Agents Chemother. 2001; 45: 1930–1933. https://doi.org/10.1128/AAC.45.6.1930-1933.2001 PMID: 11353657

23. Favre-Bonté S, Köhler T, Van Delden C. Biofilm formation by *Pseudomonas aeruginosa*: role of the C4-HSL cell-to-cell signal and inhibition by azithromycin. J Antimicrob Chemother. 2003; 52: 598–604. https://doi.org/10.1093/jac/dkg397 PMID: 12951348

24. Gillis RJ, Iglewski BH. Azithromycin retards *Pseudomonas aeruginosa* biofilm formation. J Clin Microbiol. 2004; 42: 5842–5845. https://doi.org/10.1128/JCM.42.12.5842-5845.2004 PMID: 15583321

25. Nalca Y, Jänsch L, Bredenbruch F, Geffers R, Buer J, Häussler S. Quorum-sensing antagonistic activities of azithromycin in *Pseudomonas aeruginosa* PAO1: a global approach. Antimicrob Agents Chemother. 2006; 50: 1680–1688. https://doi.org/10.1128/AAC.50.5.1680-1688.2006 PMID: 16641435

26. Skindersoe ME, Alhede M, Phipps R, Yang L, Jensen PO, Rasmussen TB, et al. Effects of antibiotics on quorum sensing in *Pseudomonas aeruginosa*. Antimicrob Agents Chemother. 2008; 52: 3648–3663. https://doi.org/10.1128/AAC.01230-07 PMID: 18644954

27. Kai T, Tateda K, Kimura S, Ishii Y, Ito H, Yoshida H, et al. A low concentration of azithromycin inhibits the mRNA expression of N-acyl homoserine lactone synthesis enzymes, upstream of *lasI* or *rhlI*, in *Pseudomonas aeruginosa*. Pulm Pharmacol Ther. 2009; 22: 483–486. https://doi.org/10.1016/j.pupt.2009.04.004 PMID: 19393329

28. Imperi F, Leoni L, Visca P. Antivirulence activity of azithromycin in *Pseudomonas aeruginosa*. Front Microbiol. 2014; 5: 10. https://doi.org/10.3389/fmicb.2014.00010 PMID: 24523718

29. Swatton JE, Davenport PW, Maunders EA, Griffin JL, Lilley KS, Welch M. Impact of azithromycin on the quorum sensing-controlled proteome of *Pseudomonas aeruginosa*. PLoS ONE. 2016; 11: e0147698. https://doi.org/10.1371/journal.pone.0147698 PMID: 26808156

30. Hassett DJ, Ma JF, Elkins JG, McDermott TR, Ochsner UA, West SE, et al. Quorum sensing in *Pseudomonas aeruginosa* controls expression of catalase and superoxide dismutase genes and mediates biofilm susceptibility to hydrogen peroxide. Mol Microbiol. 1999; 34: 1082–1093. https://doi.org/10.1046/j.1365-2958.1999.01672.x PMID: 10594832

31. Retsema J, Girard A, Schelkly W, Manousos M, Anderson M, Bright G, et al. Spectrum and mode of action of azithromycin (CP-62,993), a new 15-membered-ring macrolide with improved potency against Gram-negative organisms. Antimicrob Agents Chemother. 1987; 31: 1939–1947. https://doi.org/10.1128/AAC.31.12.1939 PMID: 2449865

32. Kannan K, Mankin AS. Macrolide antibiotics in the ribosome exit tunnel: species-specific binding and action. Ann N Y Acad Sci. 2011; 1241: 33–47. https://doi.org/10.1111/j.1749-6632.2011.06315.x PMID: 22191525

33. Kannan K, Vázquez-Laslop N, Mankin AS. Selective protein synthesis by ribosomes with a drug-obstructed exit tunnel. Cell. 2012; 151: 508–520. https://doi.org/10.1016/j.cell.2012.09.018 PMID: 23101624

34. Hansen JL, Ippolito JA, Ban N, Nissen P, Moore PB, Steitz TA. The Structures of four macrolide antibiotics bound to the large ribosomal subunit. Mol Cell. 2002; 10: 117–128. https://doi.org/10.1016/s1097-2765(02)00570-1 PMID: 12150912

35. Sothiselvam S, Liu B, Han W, Ramu H, Klepacki D, Atkinson GC, et al. Macrolide antibiotics allosterically predispose the ribosome for translation arrest. Proc Natl Acad Sci USA. 2014; 111: 9804–9809. https://doi.org/10.1073/pnas.1403586111 PMID: 24961372

36. McGary K, Nudler E. RNA polymerase and the ribosome: the close relationship. Curr Opin Microbiol. 2013; 16: 112–117. https://doi.org/10.1016/j.mib.2013.01.010 PMID: 23433801

37. Proshkin S, Rahmouni AR, Mironov A, Nudler E. Cooperation between translating ribosomes and RNA polymerase in transcription elongation. Science. 2010; 328: 504–508. https://doi.org/10.1126/science.1184939 PMID: 20413502

38. Fan H, Conn AB, Williams PB, Diggs S, Hahm J, Gamper HB, et al. Transcription-translation coupling: direct interactions of RNA polymerase with ribosomes and ribosomal subunits. Nucleic Acids Res. 2017; 45: 11043–11055. https://doi.org/10.1093/nar/gkx719 PMID: 28977553

39. Conn AB, Diggs S, Tam TK, Blaha GM. Two Old Dogs, One New Trick: A review of RNA polymerase and ribosome interactions during transcription-translation coupling. Int J of Mol Sci. 2019;20. https://doi.org/10.3390/ijms20102595 PMID: 31137816

40. Dar D, Shamir M, Mellin JR, Koutero M, Stern-Ginossar N, Cossart P, et al. Term-seq reveals abundant ribo-regulation of antibiotics resistance in bacteria. Science. 2016; 352: aad9822–aad9822. https://doi.org/10.1126/science.aad9822 PMID: 27120414

41. Tandonnet S, Torres TT. Traditional versus 3' RNA-seq in a non-model species. Genomics Data. 2017; 11: 9–16. https://doi.org/10.1016/j.gdata.2016.11.002 PMID: 27909684

42. Ma F, Fuqua BK, Hasin Y, Yukhtman C, Vulpe CD, Lusis AJ, et al. A comparison between whole transcript and 3' RNA sequencing methods using Kapa and Lexogen library preparation methods. BMC Genomics. 2019; 20: 9. https://doi.org/10.1186/s12864-018-5393-3 PMID: 30616562

43. Wang X N MPA, Jeon HJ, Lee Y, He J, Adhya S, et al. Processing generates 3' ends of RNA masking transcription termination events in prokaryotes. Proc Natl Acad Sci USA. 2019; 116: 4440–4445. https://doi.org/10.1073/pnas.1813181116 PMID: 30782818

44. Grylak-Mielnicka A, Bidnenko V, Bardowski J, Bidnenko E. Transcription termination factor Rho: a hub linking diverse physiological processes in bacteria. Microbiology. 2016; 162: 433–447. https://doi.org/10.1099/mic.0.000244 PMID: 26796109

45. Roberts JW. Mechanisms of Bacterial Transcription Termination. J Mol Biol. 2019; 431: 4030–4039. https://doi.org/10.1016/j.jmb.2019.04.003 PMID: 30978344

46. Henkin TM, Yanofsky C. Regulation by transcription attenuation in bacteria: how RNA provides instructions for transcription termination/antitermination decisions. Bioessays. 2002; 24: 700–707. https://doi.org/10.1002/bies.10125 PMID: 12210530

47. Merino E, Yanofsky C. Transcription attenuation: a highly conserved regulatory strategy used by bacteria. Trends in Genetics. 2005; 21: 260–264. https://doi.org/10.1016/j.tig.2005.03.002 PMID: 15851059

48. Abduljalil JM. Bacterial riboswitches and RNA thermometers: Nature and contributions to pathogenesis. Noncoding RNA Res. 2018; 3: 54–63. https://doi.org/10.1016/j.ncrna.2018.04.003 PMID: 30159440

49. Naville M, Gautheret D. Transcription attenuation in bacteria: theme and variations. Brief Funct Genomic Proteomic. 2009; 8: 482–492. https://doi.org/10.1093/bfgp/elp025 PMID: 19651704

50. Kortmann J, Narberhaus F. Bacterial RNA thermometers: molecular zippers and switches. Nat Rev Microbiol. 2012; 10: 255–265. https://doi.org/10.1038/nrmicro2730 PMID: 22421878

51. Irnov I, Winkler WC. A regulatory RNA required for antitermination of biofilm and capsular polysaccharide operons in Bacillales. Mol Microbiol. 2010; 76: 559–575. https://doi.org/10.1111/j.1365-2958.2010.07131.x PMID: 20374491

52. Disney MD, Dwyer BG, Childs-Disney JL. Drugging the RNA World. Cold Spring Harb Perspect Biol. 2018; 10: a034769. https://doi.org/10.1101/cshperspect.a034769 PMID: 30385607

53. Nshogozabahizi JC, Aubrey KL, Ross JA, Thakor N. Applications and limitations of regulatory RNA elements in synthetic biology and biotechnology. J Appl Microbiol. 2019; 127: 968–984. https://doi.org/10.1111/jam.14270 PMID: 30927378

54. Etzel M, Mörl M. Synthetic riboswitches: From plug and pray toward plug and play. Biochemistry. 2017; 56: 1181–1198. https://doi.org/10.1021/acs.biochem.6b01218 PMID: 28206750

55. Borges A, Simões M, Todorović TR, Filipović NR, García-Sosa AT. Cobalt complex with thiazole-based ligand as new *Pseudomonas aeruginosa* quorum quencher, biofilm inhibitor and virulence attenuator. Molecules. 2018; 23: 1385. https://doi.org/10.3390/molecules23061385 PMID: 29890626

56. Johansson J, Mandin P, Renzoni A, Chiaruttini C, Springer M, Cossart P. An RNA thermosensor controls expression of virulence genes in *Listeria monocytogenes*. Cell. 2002; 110: 551–561. https://doi.org/10.1016/s0092-8674(02)00905-4 PMID: 12230973

57. Warrier I, Ram-Mohan N, Zhu Z, Hazery A, Echlin H, Rosch J, et al. The Transcriptional landscape of *Streptococcus pneumoniae* TIGR4 reveals a complex operon architecture and abundant riboregulation critical for growth and virulence. PLoS Pathog. 2018; 14: e1007461. https://doi.org/10.1371/journal.ppat.1007461 PMID: 30517198

58. Martin M. Cutadapt removes adapter sequences from high-throughput sequencing reads. EMBnet-journal. 2011; 17: 10–12. https://doi.org/10.14806/ej.17.1.200

59. Langmead Ben, Salzberg SL. Fast gapped-read alignment with Bowtie 2. Nat Methods. 2012; 9: 357–359. https://doi.org/10.1038/nmeth.1923 PMID: 22388286

60. Quinlan AR, Hall IM. BEDTools: a flexible suite of utilities for comparing genomic features. Bioinformatics. 2010; 26: 841–842. https://doi.org/10.1093/bioinformatics/btq033 PMID: 20110278

61. Naville M, Ghuillot-Gaudeffroy A, Marchais A, Gautheret D. ARNold: a web tool for the prediction of Rho-independent transcription terminators. RNA Biol. 2011; 8: 11–13. https://doi.org/10.4161/rna.8.1.13346 PMID: 21282983

62. Freese NH, Norris DC, Loraine AE. Integrated genome browser: visual analytics platform for genomics. Bioinformatics. 2016; 32: 2089–2095. https://doi.org/10.1093/bioinformatics/btw069 PMID: 27153568

63. Wurtzel O, Yoder-Himes DR, Han K, Dandekar AA, Edelheit S, Greenberg EP, et al. The single-nucleotide resolution transcriptome of *Pseudomonas aeruginosa* grown in body temperature. PLoS Pathog. 2012; 8: e1002945. https://doi.org/10.1371/journal.ppat.1002945 PMID: 23028334

64. Kent WJ, Sugnet CW, Furey TS, Roskin KM, Pringle TH, Zahler AM, et al. The human genome browser at UCSC. Genome Res. 2002; 12: 996–1006. https://doi.org/10.1101/gr.229102 PMID: 12045153

65. Love MI, Huber W, Anders S. Moderated estimation of fold change and dispersion for RNA-seq data with DESeq2. BioMed Central; 2014; 15: 1–21. https://doi.org/10.1186/s13059-014-0550-8 PMID: 25516281

66. Mukherjee S, Sengupta S. Riboswitch Scanner: an efficient pHMM-based web-server to detect riboswitches in genomic sequences. Bioinformatics. 2016; 32: 776–778. https://doi.org/10.1093/bioinformatics/btv640 PMID: 26519506

67. Singh P, Bandyopadhyay P, Bhattacharya S, Krishnamachari A, Sengupta S. Riboswitch detection using profile hidden Markov models. BMC Bioinformatics. 2009; 10: 325–13. https://doi.org/10.1186/1471-2105-10-325 PMID: 19814811

68. Griffiths-Jones S, Bateman A, Marshall M, Khanna A, Eddy SR. Rfam: an RNA family database. Nucleic Acids Res. 2003; 31: 439–441. https://doi.org/10.1093/nar/gkg006 PMID: 12520045

69. Millman A, Dar D, Shamir M, Sorek R. Computational prediction of regulatory, premature transcription termination in bacteria. Nucleic Acids Res. 2017; 45: 886–893. https://doi.org/10.1093/nar/gkw749 PMID: 27574119

70. Whiteley M, Parsek MR, Greenberg EP. Regulation of quorum sensing by RpoS in *Pseudomonas aeruginosa*. J Bacteriol. 2000; 182: 4356–4360. https://doi.org/10.1128/JB.182.15.4356-4360.2000 PMID: 10894749

71. Schuster M, Hawkins AC, Harwood CS, Greenberg EP. The *Pseudomonas aeruginosa* RpoS regulon and its relationship to quorum sensing. Mol Microbiol. 2004; 51: 973–985. https://doi.org/10.1046/j.1365-2958.2003.03886.x PMID: 14763974

72. Potvin E, Sanschagrin F, Levesque RC. Sigma factors in *Pseudomonas aeruginosa*. FEMS Microbiol Rev. 2008; 32: 38–55. https://doi.org/10.1111/j.1574-6976.2007.00092.x PMID: 18070067

73. Erickson DL, Lines JL, Pesci EC, Venturi V, Storey DG. *Pseudomonas aeruginosa* relA contributes to virulence in *Drosophila melanogaster*. Infect Immun. 2004; 72: 5638–5645. https://doi.org/10.1128/IAI.72.10.5638-5645.2004 PMID: 15385461

74. Rompf A, Hungerer C, Hoffmann T, Lindenmeyer M, Römling U, Gross U, et al. Regulation of *Pseudomonas aeruginosa hemF* and *hemN* by the dual action of the redox response regulators Anr and Dnr. Mol Microbiol. 1998; 29: 985–997. https://doi.org/10.1046/j.1365-2958.1998.00980.x PMID: 9767567

75. Hammond JH, Dolben EF, Smith TJ, Bhuju S, Hogan DA. Links between Anr and quorum sensing in *Pseudomonas aeruginosa* biofilms. J Bacteriol. 2015; 197: 2810–2820. https://doi.org/10.1128/JB.00182-15 PMID: 26078448

76. Pérez-Martínez I, Haas D. Azithromycin inhibits expression of the GacA-dependent small RNAs RsmY and RsmZ in *Pseudomonas aeruginosa*. Antimicrob Agents Chemother. 2011; 55: 3399–3405. https://doi.org/10.1128/AAC.01801-10 PMID: 21537014

77. Lu C-D, Yang Z, Li W. Transcriptome analysis of the ArgR regulon in *Pseudomonas aeruginosa*. J Bacteriol. 2004; 186: 3855–3861. https://doi.org/10.1128/JB.186.12.3855-3861.2004 PMID: 15175299

78. Li W, Lu C-D. Regulation of carbon and ntrogen utilization by CbrAB and NtrBC two-Component systems in *Pseudomonas aeruginosa*. J Bacteriol. 2007; 189: 5413–5420. https://doi.org/10.1128/JB.00432-07 PMID: 17545289

79. Liang H, Deng X, Ji Q, Sun F, Shen T, He C. The *Pseudomonas aeruginosa* global regulator VqsR directly inhibits QscR to control quorum-sensing and virulence gene expression. J Bacteriol. 2012; 194: 3098–3108. https://doi.org/10.1128/JB.06679-11 PMID: 22505688

80. Poole K, Hay T, Gilmour C, Fruci M. The aminoglycoside resistance-promoting AmgRS envelope stress-responsive two-component system in Pseudomonas aeruginosa is zinc-activated and protects

cells from zinc-promoted membrane damage. Microbiology. 2019; 165: 563–571. https://doi.org/10.1099/mic.0.000787 PMID: 30835196

81. Persky NS, Ferullo DJ, Cooper DL, Moore HR, Lovett ST. The ObgE/CgtA GTPase influences the stringent response to amino acid starvation in *Escherichia coli*. Molecular Microbiol. 2009; 73: 253–266. https://doi.org/10.1111/j.1365-2958.2009.06767.x PMID: 19555460

82. Verstraeten N, Knapen WJ, Kint CI, Liebens V, Van den Bergh B, Dewachter L, et al. Obg and membrane depolarization are part of a microbial bet-hedging strategy that leads to antibiotic tolerance. Mol Cell. 2015; 59: 9–21. https://doi.org/10.1016/j.molcel.2015.05.011 PMID: 26051177

83. Lizewski SE, Schurr JR, Jackson DW, Frisk A, Carterson AJ, Schurr MJ. Identification of AlgR-regulated genes in *Pseudomonas aeruginosa* by use of microarray analysis. J Bacteriol. 2004; 186: 5672–5684. https://doi.org/10.1128/JB.186.17.5672-5684.2004 PMID: 15317771

84. Mavrodi DV, Bonsall RF, Delaney SM, Soule MJ, Phillips G, Thomashow LS. Functional analysis of genes for biosynthesis of pyocyanin and phenazine-1-carboxamide from *Pseudomonas aeruginosa* PAO1. J Bacteriol. 2001; 183: 6454–6465. https://doi.org/10.1128/JB.183.21.6454-6465.2001 PMID: 11591691

85. Casilag F, Lorenz A, Krueger J, Klawonn F, Weiss S, Häussler S, et al. The LasB elastase of *Pseudomonas aeruginosa* acts in concert with alkaline protease AprA to prevent flagellin-mediated immune recognition. Infect Immun. 2016; 84: 162–171. https://doi.org/10.1128/IAI.00939-15 PMID: 26502908

86. Rao J, Elliott MR, Leitinger N, Jensen RV, Goldberg JB, Amin AR. RahU: an inducible and functionally pleiotropic protein in *Pseudomonas aeruginosa* modulates innate immunity and inflammation in host cells. Cell Immunol. 2011; 270: 103–113. https://doi.org/10.1016/j.cellimm.2011.05.012 PMID: 21704311

87. Belete B, Lu H, Wozniak DJ. *Pseudomonas aeruginosa* AlgR regulates type IV pilus biosynthesis by activating transcription of the fimU-pilVWXY1Y2E operon. J Bacteriol. 2008; 190: 2023–2030. https://doi.org/10.1128/JB.01623-07 PMID: 18178737

88. Goltermann L, Good L, Bentin T. Chaperonins fight aminoglycoside-induced protein misfolding and promote short-term tolerance in *Escherichia coli*. J Biol Chem. 2013; 288: 10483–10489. https://doi.org/10.1074/jbc.M112.420380 PMID: 23447537

89. Cardoso K, Gandra RF, Wisniewski ES, Osaku CA, Kadowaki MK, Felipach-Neto V, et al. DnaK and GroEL are induced in response to antibiotic and heat shock in *Acinetobacter baumannii*. J Med Microbiol. 2010; 59: 1061–1068. https://doi.org/10.1099/jmm.0.020339-0 PMID: 20576751

90. Okuda J, Yamane S, Nagata S, Kunikata C, Suezawa C, Yasuda M. The *Pseudomonas aeruginosa* dnaK gene is involved in bacterial translocation across the intestinal epithelial cell barrier. Microbiology 2017; 163: 1208–1216. https://doi.org/10.1099/mic.0.000508 PMID: 28758636

91. Déziel E, Gopalan S, Tampakaki AP, Lépine F, Padfield KE, Saucier M, et al. The contribution of MvfR to *Pseudomonas aeruginosa* pathogenesis and quorum sensing circuitry regulation: multiple quorum sensing-regulated genes are modulated without affecting *lasRI*, *rhlRI* or the production of N-acyl-L-homoserine lactones. Mol Microbiol. 2005; 55: 998–1014. https://doi.org/10.1111/j.1365-2958.2004.04448.x PMID: 15686549

92. Colvin KM, Gordon VD, Murakami K, Borlee BR, Wozniak DJ, Wong GCL, et al. The pel polysaccharide can serve a structural and protective role in the biofilm matrix of *Pseudomonas aeruginosa*. PLoS Pathog. 2011; 7: e1001264. https://doi.org/10.1371/journal.ppat.1001264 PMID: 21298031

93. Reimmann C, Beyeler M, Latifi A, Winteler H, Foglino M, Lazdunski A, et al. The global activator GacA of *Pseudomonas aeruginosa* PAO positively controls the production of the autoinducer N-butyryl-homoserine lactone and the formation of the virulence factors pyocyanin, cyanide, and lipase. Mol Microbiol. 1997; 24: 309–319. https://doi.org/10.1046/j.1365-2958.1997.3291701.x PMID: 9159518

94. Hickman JW, Tifrea DF, Harwood CS. A chemosensory system that regulates biofilm formation through modulation of cyclic diguanylate levels. Proc Natl Acad Sci USA. 2005; 102: 14422–14427. https://doi.org/10.1073/pnas.0507170102 PMID: 16186483

95. Choby JE, Skaar EP. Heme synthesis and acquisition in bacterial pathogens. J Mol Biol. 2016; 428: 3408–3428. https://doi.org/10.1016/j.jmb.2016.03.018 PMID: 27019298

96. Tribelli PM, Lujan AM, Pardo A, Ibarra JG, Fernández Do Porto D, Smania A, et al. Core regulon of the global anaerobic regulator Anr targets central metabolism functions in *Pseudomonas* species. Sci Rep. 2019; 9: 9065–13. https://doi.org/10.1038/s41598-019-45541-0 PMID: 31227753

97. da Silva DP, Matwichuk ML, Townsend DO, Reichhardt C, Lamba D, Wozniak DJ, et al. The *Pseudomonas aeruginosa* lectin LecB binds to the exopolysaccharide Psl and stabilizes the biofilm matrix. Nat Commun. 2019; 10: 1–11. https://doi.org/10.1038/s41467-018-07882-8 PMID: 30602773

98. Winkler WC, Breaker RR. Regulation of bacterial gene expression by riboswitches. Annu Rev Microbiol. 2005; 59: 487–517. https://doi.org/10.1146/annurev.micro.59.030804.121336 PMID: 16153177

99. Wilson SA, Wachira SJ, Norman RA, Pearl LH, Drew RE. Transcription antitermination regulation of the *Pseudomonas aeruginosa* amidase operon. The EMBO Journal. 1996; 15: 5907–5916. https://doi.org/10.1002/j.1460-2075.1996.tb00977.x PMID: 8918468

100. Ochsner UA, Reiser J. Autoinducer-mediated regulation of rhamnolipid biosurfactant synthesis in *Pseudomonas aeruginosa*. Proc Natl Acad Sci USA. 1995; 92: 6424–6428. https://doi.org/10.1073/pnas.92.14.6424 PMID: 7604006

101. Fu Y, Deiorio-Haggar K, Anthony J, Meyer MM. Most RNAs regulating ribosomal protein biosynthesis in *Escherichia coli* are narrowly distributed to Gammaproteobacteria. Nucleic Acids Res. 2013; 41: 3491–3503. https://doi.org/10.1093/nar/gkt055 PMID: 23396277

102. Olekhnovich I, Gussin GN. Effects of mutations in the *Pseudomonas putida miaA* gene: regulation of the *trpE* and *trpGDC* operons in *P. putida* by attenuation. J Bacteriol. 2001; 183: 3256–3260. https://doi.org/10.1128/JB.183.10.3256-3260.2001 PMID: 11325956

103. Thomason MK, Voichek M, Dar D, Addis V, Fitzgerald D, Gottesman S, et al. A *rhlI* 5′ UTR-derived sRNA regulates RhlR-dependent quorum sensing in *Pseudomonas aeruginosa*. mBio. 2019; 10: 43. https://doi.org/10.1128/mBio.02253-19 PMID: 31594819

104. Gilbert KB, Kim TH, Gupta R, Greenberg EP, Schuster M. Global position analysis of the *Pseudomonas aeruginosa* quorum-sensing transcription factor LasR. Mol Microbiol. 2009; 73: 1072–1085. https://doi.org/10.1111/j.1365-2958.2009.06832.x PMID: 19682264

105. Mouneimné H, Robert J, Jarlier V, Cambau E. Type II topoisomerase mutations in ciprofloxacin-resistant strains of *Pseudomonas aeruginosa*. Antimicrob Agents Chemother. 1999; 43: 62–66. https://doi.org/10.1128/AAC.43.1.62 PMID: 9869566

106. Dages S, Dages K, Zhi X, Leng F. Inhibition of the *gyrA* promoter by transcription-coupled DNA supercoiling in *Escherichia coli*. Sci Rep. 2018; 8: 1–9. https://doi.org/10.1038/s41598-017-17765-5 PMID: 29311619

107. Kaguni JM. The macromolecular machines that duplicate the *Escherichia coli* chromosome as targets for drug discovery. Antibiotics. 2018; 7: 23. https://doi.org/10.3390/antibiotics7010023 PMID: 29538288

108. Friedman L, Kolter R. Genes involved in matrix formation in *Pseudomonas aeruginosa* PA14 biofilms. Mol Microbiol. 2004; 51: 675–690. https://doi.org/10.1046/j.1365-2958.2003.03877.x PMID: 14731271

109. Dana A, Tuller T. The effect of tRNA levels on decoding times of mRNA codons. Nucleic Acids Res. 2014; 42: 9171–9181. https://doi.org/10.1093/nar/gku646 PMID: 25056313

110. Buskirk AR, Green R. Ribosome pausing, arrest and rescue in bacteria and eukaryotes. Philos Trans R Soc Lond., B, 2017; 372: 20160183. https://doi.org/10.1098/rstb.2016.0183 PMID: 28138069

111. Rodnina MV. Translation in prokaryotes. Cold Spring Harb Perspect Biol. 2018; 10: a032664. https://doi.org/10.1101/cshperspect.a032664 PMID: 29661790

112. Zhu M, Mori M, Hwa T, Dai X. Disruption of transcription–translation coordination in *Escherichia coli* leads to premature transcriptional termination. Nat Microbiol. 2019; 4: 2347–2356. https://doi.org/10.1038/s41564-019-0543-1 PMID: 31451774

113. Davis AR, Gohara DW, Yap M-NF. Sequence selectivity of macrolide-induced translational attenuation. Proc Natl Acad Sci USA. 2014; 111: 15379–15384. https://doi.org/10.1073/pnas.1410356111 PMID: 25313041

114. Vázquez-Laslop N, Mankin AS. How macrolide antibiotics work. Trends Biochem Sci. 2018; 43: 668–684. https://doi.org/10.1016/j.tibs.2018.06.011 PMID: 30054232

115. Linares JF, Gustafsson I, Baquero F, Martinez JL. Antibiotics as intermicrobial signaling agents instead of weapons. Proc Natl Acad Sci USA. 2006; 103: 19484–19489. https://doi.org/10.1073/pnas.0608949103 PMID: 17148599

116. Sedlyarova N, Shamovsky I, Bharati BK, Epshtein V, Chen J, Gottesman S, et al. sRNA-mediated control of transcription termination in *E. coli*. Cell. 2016; 167: 111–121.e13. https://doi.org/10.1016/j.cell.2016.09.004 PMID: 27662085

117. Deana A, Belasco JG. Lost in translation: the influence of ribosomes on bacterial mRNA decay. Genes Dev. 2005; 19: 2526–2533. https://doi.org/10.1101/gad.1348805 PMID: 16264189

118. Iost I, Dreyfus M. The stability of *Escherichia coli lacZ* mRNA depends upon the simultaneity of its synthesis and translation. The EMBO J. 1995; 14: 3252–3261. https://doi.org/10.1002/j.1460-2075.1995.tb07328.x PMID: 7542588

119. Sunohara T, Jojima K, Tagami H, Inada T, Aiba H. Ribosome stalling during translation elongation induces cleavage of mRNA being translated in *Escherichia coli*. J Biol Chem. 2004; 279: 15368–15375. https://doi.org/10.1074/jbc.M312805200 PMID: 14744860

120. Kambara TK, Ramsey KM, Dove SL. Pervasive targeting of nascent transcripts by Hfq. Cell Rep. 2018; 23: 1543–1552. https://doi.org/10.1016/j.celrep.2018.03.134 PMID: 29719264

121. Sandler P, Weisblum B. Erythromycin-induced stabilization of *ermA* messenger RNA in *Staphylococcus aureus* and *Bacillus subtilis*. J Mol Biol. 1988; 203: 905–915. https://doi.org/10.1016/0022-2836 (88)90116-7 PMID: 2463370

122. Bechhofer DH, Zen KH. Mechanism of erythromycin-induced *ermC* mRNA stability in *Bacillus subtilis*. J Bacteriol. 1989; 171: 5803–5811. https://doi.org/10.1128/jb.171.11.5803-5811.1989 PMID: 2478520

123. Gödeke J, Pustelny C, Häussler S. Recycling of peptidyl-tRNAs by peptidyl-tRNA hydrolase counteracts azithromycin-mediated effects on *Pseudomonas aeruginosa*. Antimicrob Agents Chemother. 2013; 57: 1617–1624. https://doi.org/10.1128/AAC.02582-12 PMID: 23318806

124. Raina M, Ibba M. tRNAs as regulators of biological processes. Front Genet. 2014; 5: 22901. https://doi.org/10.3389/fgene.2014.00171 PMID: 24966867

125. Feng B, Mandava CS, Guo Q, Wang J, Cao W, Li N, et al. Structural and functional insights into the mode of action of a universally conserved Obg GTPase. Petsko GA, editor. PLoS Biol. 2014; 12: e1001866. https://doi.org/10.1371/journal.pbio.1001866 PMID: 24844575

126. Larson MH, Mooney RA, Peters JM, Windgassen T, Nayak D, Gross CA, et al. A pause sequence enriched at translation start sites drives transcription dynamics *in vivo*. Science. 2014; 344: 1042–1047. https://doi.org/10.1126/science.1251871 PMID: 24789973

127. Gourse RL, Chen AY, Gopalkrishnan S, Sanchez-Vazquez P, Myers A, Ross W. Transcriptional responses to ppGpp and DksA. Annu Rev Microbiol. 2018. https://doi.org/10.1146/annurev-micro-090817-062444 PMID: 30200857

128. Dersch P, Khan MA, Mühlen S, Görke B. Roles of regulatory RNAs for antibiotic resistance in bacteria and their potential value as novel drug targets. Front Microbiol. 2017; 8: 803. https://doi.org/10.3389/fmicb.2017.00803 PMID: 28529506

129. Mulhbacher J, Brouillette E, Allard M, Fortier L-C, Malouin F, Lafontaine DA. Novel riboswitch ligand analogs as selective inhibitors of guanine-related metabolic pathways. PLoS Pathog. 2010; 6: e1000865. https://doi.org/10.1371/journal.ppat.1000865 PMID: 20421948

130. Ster C, Allard M, Boulanger S, Lamontagne Boulet M, Mulhbacher J, Lafontaine DA, et al. Experimental treatment of *Staphylococcus aureus* bovine intramammary infection using a guanine riboswitch ligand analog. J Dairy Sci. 2013; 96: 1000–1008. https://doi.org/10.3168/jds.2012-5890 PMID: 23245959

131. CLSI. Performance standards for antimicrobial susceptibility testing. Wayne, PA: Clinical and Laboratory Standards Institute; 2019

132. Silke JR, Wei Y, Xia X. RNA-Seq-based analysis reveals heterogeneity in mature 16S rRNA 3' termini and extended anti-Shine-Dalgarno motifs in bacterial species. G3 (Bethesda). 2018; 8: 3973–3979. https://doi.org/10.1534/g3.118.200729 PMID: 30355764

133. Kaczanowska M, Rydén-Aulin M. Ribosome biogenesis and the translation process in *Escherichia coli*. Microbiol Mol Biol Rev. 2007; 71: 477–494. https://doi.org/10.1128/MMBR.00013-07 PMID: 17804668

134. Turnbough CL, Switzer RL. Regulation of pyrimidine biosynthetic gene expression in bacteria: Repression without repressors. Microbiol Mol Biol Rev. 2008; 72(2): 266–300. https://doi.org/10.1128/MMBR.00001-08 PMID: 18535147

135. Du H, Tarpey R, Babitzke P. The *trp* RNA-binding attenuation protein regulates TrpG synthesis by binding to the *trpG* ribosome binding site of *Bacillus subtilis*. J Bacteriol. 1997; 179: 2582–2586. https://doi.org/10.1128/jb.179.8.2582-2586.1997 PMID: 9098056